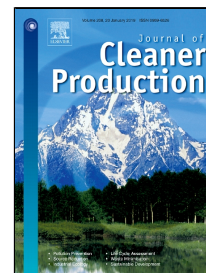


# Accepted Manuscript

Geopolymer for use in heavy metals adsorption, and advanced oxidative processes: a critical review



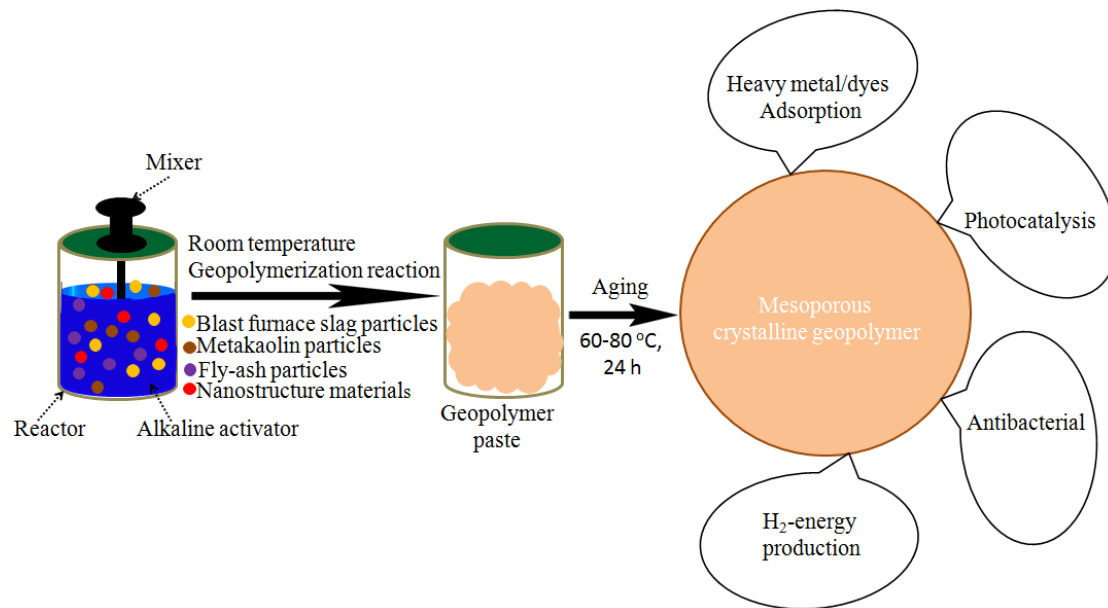
Sefiu Abolaji Rasaki, Zhang Bingxue, Rohiverth Guarecuco, Tiju Thomas, Yang Minghui

PII: S0959-6526(18)33855-1  
DOI: 10.1016/j.jclepro.2018.12.145  
Reference: JCLP 15203  
To appear in: *Journal of Cleaner Production*  
Received Date: 25 September 2018  
Accepted Date: 15 December 2018

Please cite this article as: Sefiu Abolaji Rasaki, Zhang Bingxue, Rohiverth Guarecuco, Tiju Thomas, Yang Minghui, Geopolymer for use in heavy metals adsorption, and advanced oxidative processes: a critical review, *Journal of Cleaner Production* (2018), doi: 10.1016/j.jclepro.2018.12.145

This is a PDF file of an unedited manuscript that has been accepted for publication. As a service to our customers we are providing this early version of the manuscript. The manuscript will undergo copyediting, typesetting, and review of the resulting proof before it is published in its final form. Please note that during the production process errors may be discovered which could affect the content, and all legal disclaimers that apply to the journal pertain.

## Graphical abstract (TOC)



Resultant Word count = 14,760

## Geopolymer for use in heavy metals adsorption, and advanced oxidative processes: a critical review

Sefiu Abolaji Rasaki,<sup>a,e</sup> Zhang Bingxue,<sup>a</sup> Rohiverth Guarecuco,<sup>b</sup> Tiju Thomas,<sup>\*c,d</sup> and Yang Minghui<sup>a\*</sup>

<sup>a</sup>Solid State functional Materials Research Laboratory, Ningbo Institute of Materials Technology and Engineering (NIMTE), Chinese Academy of Sciences (CAS), 315201, Ningbo China.

<sup>b</sup>Department of Chemistry & Chemical Biology Cornell University, Ithaca, New York 14853, United States.

<sup>c</sup>Department of Metallurgical and Materials Engineering, Indian Institute of Technology Madras Adyar, Chennai 600036, Tamil Nadu, India

<sup>d</sup>Indian Solar Energy Harnessing Center (ISEHC) – An Energy Consortium, Indian Institute of Technology Madras Adyar, Chennai 600036, Tamil Nadu, India

<sup>e</sup>University of Chinese Academy of Science, Beijing 100049, China.

\*Corresponding author email: [myang@nimte.ac.cn](mailto:myang@nimte.ac.cn), [tijuthomas@iitm.ac.in](mailto:tijuthomas@iitm.ac.in)

### Abstract

Geopolymer is a ceramic material, most often amorphous; finds applications in fire- and heat-resistant coatings and adhesives, medicines, refractory ceramics and binders, and manufacturing of radioactive waste container. Over the last decade, new cement based on geopolymers has been developed. Most relevant to this review is the fact that its porous nature and chemical similarity to zeolites is being employed for applications pertaining to wastewater treatment. Most of the work has been on the adsorptive treatment of water. However, using chemical reasoning and literature available we show that geopolymers have relevance for further activity on additional areas of relevance to waste water treatment such as photocatalysis, disinfection, and H<sub>2</sub>-energy production from waste water etc. These applications would depend strongly on the properties of geopolymers, which in turn would rely on the precursors employed and the synthetic methods used. The relevance of geopolymers for cleaner production is also highlighted. The use of fly ashes and metakaolin composites for the fabrication and surface tailoring of geopolymers (perhaps using relevant surfactants) is suggested as a plausible step in the right direction. Given the critical analysis of the state of the art, and the plausible directions identified, this article will benefit environmental scientists, engineers and chemists interested in deploying geopolymers for environmental remediation purposes. However moving forward, barriers are

32 to be anticipated for the large scale implementation of geopolymers. Several barriers (e.g. legal,  
33 economical, technocrats and synthetic challenges) that are likely to hinder future research and translation  
34 are highlighted.

35 *Keywords: Metakaolin-geopolymer; Fly ash; adsorbent; photocatalytic support; antibacterial activity*

## 36 **1. Introduction**

37 Heavy metal removal and organic molecule degradation from wastewater have become a major topic  
38 of the public interest, due to their relevance to health and environment. Heavy metal and hazardous  
39 organic molecules are known to be toxic and a precursor to ill-health of the populace (Jaishankar et al.,  
40 2014). They are primarily released into the environment through human/industrial activities (Azimi et al.,  
41 2017). Hence research on multifunctional materials which relates to simultaneous environmental  
42 remediation and energy production are relevant to contemporary technologies connected with cleaner  
43 production.

44 Geopolymers are a promising category of materials, for the removal of toxic substances from  
45 industrial and household effluents. It is usually prepared from a rather simple and eco-friendly reaction  
46 between an alkali such as NaOH/Na<sub>2</sub>SiO<sub>3</sub> or KOH; and Al and Si source (s), making it a material  
47 amenable to clean production. Geopolymers obtained thus are often applied for the removal of metal ions  
48 such as Cs<sup>+</sup>, Pb<sup>2+</sup>, Cd<sup>2+</sup> etc. from wastewater. Geopolymers have come a long way, since their first  
49 discovery four decades ago (Davidovits, 1976). It has gained attention primarily because of the ease with  
50 which it can be synthesized with little or zero emission of green house gases (CO<sub>2</sub>, SO<sub>2</sub>, NO<sub>x</sub> etc.) (Noor  
51 ul et al., 2016). This coupled with its properties which include toughness, fire and heat resistance (i.e. its  
52 refractory nature), radiation hardness (making it relevant for radioactive waste containment) and  
53 pozzolanic action (Carsten, 2013), make geopolymers truly multifunctional.

54 In fact, plenty of industrially relevant materials have been derived through geopolymers. For  
55 instance, geopolymer-fiber composites are characterized with fire resistant properties. Several

56 geopolymer composites are deployed in metal tool coatings, and construction of airplane cabinets and  
57 buildings, in order to reduce the intensity of inferno accidents (Salwa et al., 2013). Also due to its  
58 polymeric chain-like structure that gives rise to high chemical resistance, low shrinkage, high resistance  
59 to abrasion and early mechanical strength (Aizat et al., 2015; Singh et al., 2015), geopolymers have  
60 become an emergent class of materials for the sustainable revamp of dilapidated infrastructures,  
61 sustainable reinforcement of structural amenities and reclamation of swamp environments. Geopolymers  
62 can be tailored to have highly workable properties as a result of its water retention ability, while having a  
63 shear stress of  $\sim 80$  Pa at a shear rate of  $110 \text{ s}^{-1}$  and compressive strengths of  $\sim 40$  MPa at 7 days curing  
64 ages (Geddes et al., 2018). These are also the properties that make geopolymers an important category of  
65 emerging materials for the capping and containment of nuclear wastes threats (Perera et al., 2011).

66 Geopolymers can be made from (i) fly ash (ii) clay (iii) slag, (iv) raw kaolin, and (v) metakaolin,  
67 (CĂȚĂNESCU et al., 2012; Villaquirán-Caicedo and Gutiérrez, 2015). Furthermore, in recent times, its'  
68 applications in disinfection have gained ground (Timakul et al., 2016). All these are making the system  
69 (i.e. geopolymer) of substantial interest to researchers focusing on cleaner production.

70 From the standpoint of technological applications; the major attraction of geopolymers comes from  
71 the fact that its production is readily scalable. In addition, considering the fact that it employs minerals of  
72 geological origin, the process is rendered rather green and eco-friendly. Also, geopolymer manufacturing  
73 enables beneficiation of industrial and agricultural waste (e.g. fly ash, slag, and rice husks) (Sturm et al.,  
74 2016). This has been an add-on for researchers focusing on geopolymer fabrication for infrastructure  
75 design and reclamation (Prachasaree et al., 2014). In fact, it brings about a huge reduction of both  
76 industrial and agricultural wastes, which in turn enables cleaner production systems in the manufacturing  
77 industries.

78 From a fundamental standpoint too, these compounds raise rather interesting questions. For instance,  
79 the near-complete elimination of diffusion of sequestered metal ions and avoidance of leaching related

80 problems associated with geopolymer adsorbents, raise interesting questions about their surface and  
81 structure (Cioffi et al., 2003). Structurally, geopolymers are known to involve inter-crossed linked bonds  
82 with cationic ends on the surface. It is these that allow entrapment of the radioactive and toxic metals  
83 through charge-balancing (Vu and Tran, 2018). However, the precise roles of the (a) anionic substitution  
84 into the its structure and (b) surface chemistries due to the surface cationic species(e.g.  $\text{Fe}^{3+}$ ,  $\text{Ti}^{4+}$ ,  $\text{Ca}^{2+}$ ,  
85  $\text{Al}^{3+}$  or  $\text{Si}^{4+}$ ) is not fully understood. Nonetheless, its microstructure in the nanometric scale (5-10 nm)  
86 often consists of several pores within a highly porous -Al-O-Si- repeated unit; these pores are likely to  
87 give room for ionic incorporation, substitution and balances (Duxson et al., 2007a). It may be noted here  
88 that geopolymers have been reported to show a substantial removal of heavy metals such as Cd(II),  
89 Ni(II), Pb(II) and Cu (II) (Cheng et al., 2012), and anions such as phosphate, fluoride, and radionuclide  
90 of  $^{137}\text{Cs}$  and  $^{90}\text{Sr}$ , and dyes (Ahmaruzzaman, 2010; López et al., 2013). However, it is important to note  
91 that surface redox reactions in general and origins of photoactivity remain largely open questions in the  
92 context of geopolymers. This certainly merits further investigation considering the fact that it has a  
93 relation to its disinfecting properties. In short, while geopolymers have already made it to several  
94 commercial applications; their fundamental surface chemistry and electronic structure continue to offer  
95 opportunities for further exploration. Here, we critically survey available literature to offer specific  
96 details relevant to geopolymers' physicochemical properties; especially those related to their electronic  
97 structures which are expected to enable their applications useful for water remediation (i.e.  
98 photodegradation of hazardous organic compounds, energy evolution/storage, heavy metals adsorption  
99 and antibacterial).

## 100 2. Chemistry of geopolymers

### 101 2.1 Geopolymerization of Aluminosilicate

102 Geopolymers are skeleton structures that emerge from the polycondensation of aluminosilicate  
103 materials. The reaction mechanism involved is responsible for the formation of this rigid structure; the

104 reaction involves a complete dissolution of the aluminosilicate phase in alkali solution, which in turn  
 105 produces two distinct tetrahedral ends {i.e. silicates ( $\text{SiO}_4$ ) and aluminates ( $\text{AlO}_4$ )}, connected through  
 106 oxygen atoms (Khale and Chaudhary, 2007). The typical stages for aluminosilicate framework  
 107 transformation to geopolymer solid structure are shown in Table. 1.

108 **Table 1:** Chemistry of geopolymerization for the transformation of aluminosilicate materials to solid state  
 109 geopolymers.

Reaction stage	Geopolymer phase	Reaction mechanism
(1) Aluminosilicate dissolution and separation into alumina and silicate ends	(1) poly(sialate)	$n(\text{Si}_2\text{O}_5, \text{Al}_2\text{O}_2) + n\text{H}_2\text{O} + \text{NaOH/KOH} \rightarrow n(\text{OH})_3\text{-Si-O-Al}(\text{OH})_3 + \text{Na}^+/\text{K}^+$
	(2) Poly(sialate-siloxo)	$n(\text{Si}_2\text{O}_5, \text{Al}_2\text{O}_2) + n\text{SiO}_2 + n\text{H}_2\text{O} + \text{NaOH/KOH} \rightarrow n(\text{OH})_3\text{-Si-O-Al-O-Si}(\text{OH})_3 + \text{Na}^+/\text{K}^+$
(2) Polycondensation/polymerization	(1) Poly(sialate)	$n(\text{OH})_3\text{-Si-O-Al}(\text{OH})_3 + \text{NaOH/KOH} \rightarrow (\text{Na}^+/\text{K}^+)\text{-(Si-O-Al-O-)}_n + n\text{H}_2\text{O}$
	(2) Poly(sialate-siloxo)	$n(\text{OH})_3\text{-Si-O-Al-O-Si}(\text{OH})_3 + \text{NaOH/KOH} \rightarrow (\text{Na}^+/\text{K}^+)\text{-(Si-O-Al-O-Si-O-)}_n + n\text{H}_2\text{O}$

110 *Note; \*Al: -Al-O- and \*Si:-Si-O-*

111 As shown in Table 1, two primary phases are likely to be derived depending on the ratio of  $\text{SiO}_2$  to  
 112  $\text{Al}_2\text{O}_3$  in the raw material used. For instance, the use of additional source of  $\text{SiO}_2$  {e.g. sodium silicate  
 113 ( $\text{Na}_2\text{SiO}_3$ )} together with NaOH/KOH produces poly(sialate-siloxo) framework, while pure NaOH/KOH  
 114 produces poly(sialate) framework (Srinivasan and Sivakumar, 2013). Stage 1 of the reaction involves  
 115 leaching of powder-like aluminosilicate materials inside alkaline solutions which leads to the formation  
 116 of aluminum and silicon hydroxide structure-like ends in an open chain system. The two ends can  
 117 undergo polycondensation reaction as a result of a condensation reaction between two hydroxyl groups to  
 118 release water molecules, thereby forming a long chain reaction which produces a gel-like material. The  
 119 diffusion of ionic species ( $\text{Na}^+/\text{K}^+$ ) balances ionic reaction, thereby causing polymerization reaction as  
 120 shown in reaction stage 2. At this stage, a vigorous mixing is required to ensure complete diffusion of the  
 121 alkali species, in order to prevent the formation of non-polymerized alumina and silicate ends within the  
 122 final geopolymer matrix. Exposure of the polymerized material to temperatures slightly above that of

123 ambient atmosphere will result into solid and stable geopolymer structures (Srinivasan and Sivakumar,  
124 2013). Considering the speciation of the aluminosilicate structure in alkali solution, the  $\text{Si}^{4+}$ , or  $\text{Al}^{3+}$  often  
125 coordinated with four oxygen atoms to give  $[\text{SiO}_4]^{4-}$  and  $[\text{AlO}_4]^{5-}$  respectively, which are referred to as  
126 aluminosilicate units. The ratio of the  $[\text{SiO}_4]^{4-}$  to  $[\text{AlO}_4]^{5-}$  is one of useful parameters for the  
127 determination of geopolymerization process and structural properties of the final geopolymer (Yao et al.,  
128 2009).

## 129 **2.2 Distinct features**

130 From the physicochemical standpoint, the chemical composition of geopolymer is relatively similar  
131 to zeolites. However, unlike zeolites, geopolymers have no crystalline order. In fact, they are considered  
132 amorphous (Bakharev, 2005; Duxson et al., 2007b; Khale and Chaudhary, 2007). The largely amorphous  
133 nature of geopolymers stems from the mixture of unrefined minerals (e.g. quartz, kaolin, hematite, and  
134 illite) present in it, most of which are largely non-crystalline. The phase that is dominant is that which  
135 consists of  $\text{Al}_2\text{O}_3$  and  $\text{SiO}_2$  (often present even as aluminosilicates) (Djobo et al., 2014). In fact most of  
136 the geological minerals and industrial waste containing these components (e.g.  $\text{Al}_2\text{O}_3$  and  $\text{SiO}_2$ ) are  
137 usually suitable for geopolymer synthesis (Djobo et al., 2014). Thermal annealing of these precursors  
138 (especially from geological sources) and fillers introduction (e.g. mesoporous silica) oftentimes result in a  
139 phase separation between the  $\text{Al}_2\text{O}_3$  and  $\text{SiO}_2$ , thereby yielding better crystallinity in the final product  
140 (Zahid et al., 2018). This process can in fact impact reactivity towards alkaline activators, and also result  
141 in reasonable porosity. However, it is evident that much more needs to be done for ensuring applications  
142 in catalysis, and allied areas. Simultaneous engineering of geopolymers to achieve the right combination  
143 of crystallinity, porosity, particles sizes and electrons conductivity will continue to be a relevant activity.

144 Another major point to be noted from an applied chemistry perspective is that the pozzolanic action of  
145 geopolymers is very different from that of well-known cements. In particular, calcium-silicate-hydrate  
146 (CSH) matrices do not occur in geopolymers. Regardless of this; its mechanical strength is comparable to

147 or better than that of Ordinary Portland cement (OPC), i.e. 64 MPa of geopolymer (Živica et al., 2011; Xu  
148 and Deventer, 2003), against 52.96 MPa of OPC (Živica et al., 2011; Husem, 2006). This attribute results  
149 from significant amount of SiO<sub>2</sub> (i.e. ~ 93.7%) in the geopolymer matrix (Okoye et al., 2016). In fact,  
150 considering its high adsorption capacity towards hazardous materials, high SiO<sub>2</sub> content in geopolymer  
151 often enhances its ability to separate and stabilize hazardous materials from environmental medium,  
152 respectively (López et al., 2014). Furthermore, the geopolymers offer stable support making it relevant for  
153 co-catalyst applications as well. Of particular value here are geopolymers that are derived from fly ash,  
154 metakaolin and blast furnace slag. Such geopolymers are reasonable co-catalyst or catalyst supports since  
155 they offer good intimate contact between the targeted molecules and catalyst phases owing to their  
156 properties (i.e. small particle sizes, high surface area, nanostructure surfaces, large proportion of metal  
157 oxides consisting of exposed oxygen atoms, and high SiO<sub>2</sub> content). All these are strongly related to  
158 electronic structures in the system, which oftentimes offer effective electron transfers (Fallah et al., 2015).  
159 However, further investigation into electronic properties of geopolymer is likely to be helpful in this field.  
160 In addition, these geopolymers tend to have relatively robust active sites. This stems from the fact that  
161 materials with large proportion of SiO<sub>2</sub> (such as geopolymers) oftentimes consists of high density of  
162 outer-, meso- and inner-pores (Panda et al., 2017; Wang et al., 2018) to facilitate: (I) good penetration of  
163 the targeted molecules into the catalyst system, and (II) large area for the mass transfer of both ions and  
164 electrons in the inner surface of the catalyst. Thus, the higher the SiO<sub>2</sub> content in the geopolymer matrix  
165 the better will its effective activity be, as either a co-catalyst or as a catalyst-support.

### 166 **3. Method and analysis section**

167 Given the state of the art in geopolymers research, and considering the relevance of compositional,  
168 structural and morphological modifications for achieving relevant functional properties along with  
169 poison resistance; in this review, we will focus on synthesis-properties (of relevance to water treatment)  
170 correlations of geopolymers. The following sections contain details and a critical analysis of (a) synthesis  
171 of geopolymers and the mechanisms, (b) properties of various raw materials, (c) interaction of

172 geopolymer products with water (with specifics to do with the water chemistries involved), (d)  
173 adsorption, photocatalysis, antibacterial, and H<sub>2</sub>-evolution applications of advanced geopolymers, (e) the  
174 likely ways forward. (a-e) is written by carefully sifting through literatures using content analysis  
175 approaches, and by employing careful searches performed using standard journal data bases and search  
176 engines (Science Direct and Google scholar). For catalytic applications, factors involved in electron  
177 generation and transfer from surface of geopolymers are essential. These factors can be modified in an  
178 application-specific manner using surface tailoring. The significance of powder X-ray diffractometer  
179 (PXRD) and Fourier transform infra red spectroscopy (FTIR) for the investigation of the crystallinity and  
180 existence of relevant bonds in the raw material phases prior to their use for geopolymer synthesis is  
181 highlighted based on current literature. Correlations between the Brunauer–Emmett–Teller (BET) surface  
182 area and pore volume to the synthesis methods are systematically examined based on recent results. The  
183 practices essential for deployment of geopolymer for water remediation are consistently highlighted.  
184 Post-treatment and disposal of the spent geopolymers' adsorbent/photocatalyst are usually  
185 straightforward since these systems do not leach readily.

#### 186 **4. Synthesis of geopolymers and mechanisms involved**

187 The mechanism that is currently accepted for the synthesis of geopolymers involves a  
188 polycondensation reaction between silica and alumina precursors, where a partial substitution of Si<sup>4+</sup>  
189 with Al<sup>3+</sup> takes place, followed by a complete ionic-balance with the Na<sup>+</sup>/K<sup>+</sup> of the alkaline activator  
190 (Zhuang et al., 2016). This results in an extended Al-O-Si network, which has high bond strength of  
191 ~3.02 KJ/mol. Such high values are due to the mixed and somewhat covalent bonds associated with the  
192 following pairs present in geopolymers: Al-O, Si-O and highly ionic Na-O (Hu et al., 2008; Jaarsveld et  
193 al., 2002). The relatively high ionicity associated with geopolymers has to do with the electronegativity  
194 differences that exist between the cations (Al and Si) and the anion (O) (Hu et al., 2008). The resultant  
195 network has a substantial structural strength (i.e. 30 MPa) at room temperature after ~24 h of synthesis,  
196 which is one of the hallmarks of geopolymers (Rovnanik, 2010). Nearly all kinds of geopolymers'

197 synthesis are carried out at room temperature making the process a cleaner production when compared  
198 to other similar ceramics.

199 During the synthesis, the choice of the alkaline activator plays a significant role since cation ( $\text{Na}^+$  or  $\text{K}^+$ )  
200 from alkaline solution is responsible for achieving the charge-balance of the  $\text{Al}(\text{OH})_4^-$  in the pores of the  
201 geopolymer paste (Duxson et al., 2005). As such, species with a higher ionic radius (i.e.  $\text{K}^+=1.33\text{pm}$ ) has  
202 lesser chances of penetration into the pores thereby resulting in a lot of unreacted phase (Samantasinghar  
203 and Singh, 2018). Of course, this is likely to result in a fast solidification of the final geopolymer since  
204 the reaction is taking place at the surface of the material. However, severe internal cracking, lower  
205 porosity and low compressive strength may occur when compared to system with  $\text{Na}^+$  ions (i.e. from  
206  $\text{NaOH}/\text{Na}_2\text{SiO}_3$ ), which has a smaller ionic radius of  $0.98\text{pm}$ . In fact,  $\text{Na}^+$  has better chances of deep  
207 penetration into the geopolymer pores for a complete reaction (Abdul Rahim et al., 2014). Alkaline  
208 solutions used for the synthesis offer means to determine the emergent structural, chemical and physical  
209 properties of the geopolymer as illustrated in Fig. 1 (Samantasinghar and Singh, 2018). In fact, one  
210 reasonable approach here would be to use a mixture of metal hydroxide and silicate solution, (as alkaline  
211 activator) (Ma et al., 2013), in order to increase silica content for improving the viability from the  
212 standpoint of environmental remediation and catalytic applications. For instance, when a mixture of  
213 potassium hydroxide and calcium silicate is used; poly(sialate-disiloxo) sanidine is obtained, (Zhang et  
214 al., 2008). On the other hand, sodium silicate/hydroxide yields poly(sialate) sodalite and calcium silicate  
215 yields poly(disialate) anorthite (ref: Fig. 1) (Davidovits, 1994). Likewise, potassium silicate/hydroxide  
216 yields poly(sialate-siloxo) leucite and potassium hydroxide will eventually yield poly(sialate) kalsilite  
217 frameworks (ref: Fig. 1), (Davidovits, 1994). All these show important of structural transformation based  
218 on  $\text{NaOH}$  or  $\text{KOH}$ /silicate mixing strategies. Such transformations are useful for the determination of  
219 mechanical properties and microstructure of the expected final geopolymer in accordance with the  
220 orthogonal design principle (material design and structural proposition prior the synthesis practices).  
221 Among the frameworks described above; poly(sialate) sodalites have a rigid molecular structure, which

222 is desirable for structural applications (e.g. pavement, road and building construction), due to its high  
223 compressive (Bakri et al., 2011; Hoy et al., 2016). Other structures however provide opportunities for the  
224 mechanical entrapment of toxic and hazardous substances. In summary, fundamental investigations  
225 correlating surface chemical features, initial precursors, and process parameters are essential to  
226 developing ‘functional geopolymers’ related particularly to applications of relevance to environmental  
227 applications.

#### 228 **4.1 Metakaolin precursor-derived from kaolin clay and their role in the degree of crystallinity**

229 Metakaolin, a precursor for the synthesis of geopolymers is obtained through dehydroxylation of  
230 kaolinite (also referred to as kaolin) over a temperature range of 520-650°C (Ke et al., 2018; Ogundiran  
231 and Enakerakpo, 2018; Samal et al., 2017). Metakaolin rather than kaolinite as a starting material offers  
232 unique advantages in terms of high reactivity and purity (Cheng et al., 2012; Yip et al., 2004), this  
233 oftentimes results in a geopolymer with better compressive strength, high surface area, and voluminous  
234 porous surfaces. In addition, geopolymers made using this precursor has several metal oxides including  
235  $\text{Al}_2\text{O}_3$  37.6%,  $\text{Fe}_2\text{O}_3$  0.94%,  $\text{TiO}_2$  0.8%,  $\text{MgO}$  0.24%,  $\text{K}_2\text{O}$  0.22%,  $\text{CaO}$  0.2%, and  $\text{Na}_2\text{O}$  0.13% (Strini et  
236 al., 2016; Temuujin et al., 2009). This makes this system (i.e. metakaolin based geopolymer) relevant for  
237 semiconductor catalysis applications. These materials can interact with light of relevant wavelengths,  
238 resulting in the creation of photogenerated carriers (electrons and holes). Hence, these materials can  
239 have reasonable photocatalytic activities (Strini et al., 2016; Zhang et al., 2012). Of particular note for  
240 further activity is the fact that metakaolin-based geopolymers can be tailored to exhibit crystalline  
241 phases (zeolite-like nanocrystalline) (López et al., 2014; Luukkonen et al., 2017). This is in fact  
242 achievable even through room temperature synthesis routes make it relevant for cleaner production step.  
243 Such crystallinity will increase the surface area, and the exposure of its metal oxides (Hoy et al., 2016),  
244 thereby enabling catalytic activity under visible light irradiation (i.e. wavelength 400-800 nm). With  
245 this, low cost and cleaner production of water treatment reactors/reservoirs are likely to be achieved. The  
246 properties (i.e. purity, crystallinity high surface areas, and metal oxides) make metakaolin-based  
247 geopolymers a rather interesting category (Bernal et al., 2011; Tang et al., 2016; Trivunac et al., 2016).

248 Furthermore, it offers an additional handle on the properties of the materials like making it readily  
249 relevant, through rather green chemical approaches, for applications involving nanocrystallinities (Strini et  
250 al., 2016). In all cases, the selection and characterization of clays play a vital role in benchmarking  
251 synthetic procedures. Clay with large degrees of crystalline kaolinite (ref: Fig. 2) offer opportunities to  
252 obtain reasonable quantities of metakaolin in the product, after the dehydroxylation process (Alshaaer et  
253 al., 2017; Faqir et al., 2018; Murray, 2006). In such process, significant loss of O-H and Si-O-Al bonds  
254 is often observable (Gasparini et al., 2013). In fact, good dehydroxylation and a large amount of  
255 metakaolin are often obtained in a clay containing a high proportion of kaolinite unit structures (Fig. 3a),  
256 with a silica end consists of pseudo-hexagonal, and alumina phase consists of octahedral shape in a  
257 uniform array as shown in Fig. 3b and c respectively (Murray, 2006).

258 Thermal dehydroxylation of kaolinite oftentimes leads to a structural transformation from pseudo-  
259 hexagonal/octahedral to a tetrahedral shape of highly reactive metakaolin (Černý et al., 2009; Murray,  
260 2006). Besides this, the endothermic process involved here (i.e. kaolinite dehydroxylation) implies that a  
261 large amount of energy is required to remove the chemically bonded hydroxyl group. This operation  
262 results in: (I) separation of the stacked layers of kaolinite (ref: Fig. 4a), and (II) formation of metakaolin  
263 with high crystallinity, and subsequent modification of bonding behaviors (ref: Fig. 4b and c respectively)  
264 (Seynou et al., 2016).

265 For the researchers working with kaolin based geopolymers, it is worth noting that kaolinite  
266 dehydroxylates at  $\sim 600^\circ\text{C}$  resulting in a large proportion of quartz minerals (i.e. a major constituent of  
267 metakaolin) and gives reasonable stability to the final geopolymer product (Kljajević et al., 2017; Seynou  
268 et al., 2016). In Fig. 4c, Fourier transform infra red spectroscopy analysis (FTIR) shows that  
269 dehydroxylation of -Si-O-Al- with band between  $3600$  and  $1000\text{ cm}^{-1}$  often takes place at  $600^\circ\text{C}$  (Černý et  
270 al., 2009; Masliana et al.; Seynou et al., 2016). This process often gives substantial amount of -Si-O-Al-  
271 framework structure which is a major phase of quartz (Černý et al., 2009; Masliana et al.; Seynou et al.,  
272 2016). Specifically, the presence and large amount of quartz in the metakaolin plays significant roles for

273 the formation of geopolymer with high compressive strength, for effective encapsulation of hazardous  
 274 materials (i.e. larger the amount of quartz, better is the geopolymer strength).

275 **Table 2:** Summary of various clay, kaolinite, and metakaolin-derived geopolymers with their  
 276 physicochemical properties relevant for environmental applications.

Precursor	Alkaline activator	Setting parameter	Geopolymer properties	Drawbacks	Ref.
Clay and sand	NaOH (10M)	Room temperature	Compressive strength=14.92MPa	NaOH>10% results in compressive strength decrease	(Rahman et al., 2016)
Kaolinite, and zeolitic tuff	NaOH (8.7M)	80°C, 24 h	Surface area=47.9m <sup>2</sup> g <sup>-1</sup>	Incomplete zeolitic dissolution	(Yousef et al., 2012)
Kaolinite	NaOH	At room temperature with secondary treatment in NaOH, temperature=80°C, 1 h	Compressive strength=60MPa	High content of residual water-soluble salt results in compressive strength reduction	(Alshaaer, 2013)
Kaolinite	Na <sub>2</sub> SiO <sub>3</sub> /NaOH (12M)	80°C, 1-3 days	-	High Na <sup>+</sup> dissolution causes low compressive strength	(Heah et al., 2013)
Kaolinite	NaOH (8M)	Room temperature, post treatment by steam curing increases compressive strength	-	-	(Hamaideh et al., 2014)
Metakaolin and sand	Na <sub>2</sub> SiO <sub>3</sub> /NaOH (8M)	Room temperature	Compressive strength=64MPa, Flexural strength=17.6MPa	Increase in curing temperature reduces strength	(Pelisser et al., 2013)
Metakaolin	NaOH (8M)	-	-	High curing temperature (>80°C) causes NaAlO <sub>2</sub>	(López et al., 2014)

---

dissolution, and  
low  
compressive  
strength

---

277 Appropriate choice of precursors, experimental parameters and its correlation with observed  
278 properties in the final product are likely to result in fresh avenues (ref: Table 2). This is especially true  
279 since in the context of approaches towards modifications of geopolymer properties of relevance to water  
280 remediation, there is hitherto very little known. Here, it would be of interest to note that raw clay- and  
281 kaolinite-based geopolymer use inexpensive synthetic approaches (including those with no pre-thermal  
282 treatment involved). However, such materials have less reactivity, porosity, crystallinity, and stability  
283 (Bignozzi et al., 2013; Fabbri et al., 2013; Khale and Chaudhary, 2007), making it of low interest  
284 especially in the field of heavy metal adsorption, photocatalysis and even newly emerging disinfectant  
285 applications. Hence, there is an emerging emphasis on metakaolin based geopolymers that are  
286 mesoporous, and highly crystalline (Ofer-Rozovsky et al., 2016). Nevertheless, considerable attention  
287 needs to be placed towards its alkaline activator post-dissolution which often hinders the stabilization.  
288 Here, it is believed that considerable advancements can be achieved by using industrial waste which will  
289 serve as filler to increase the stability of the final geopolymer (Lee et al., 2016; Lee et al., 2017).  
290 Coupling this with steam curing methods is likely to increase the workability of the geopolymer, which  
291 may then be pulverized for use in heavy metals' adsorption and catalysis purposes (i.e. applications  
292 involving water remediation). This is also likely to make geopolymer useful for sewage slug containment  
293 which in turn would be relevant for cleaner approaches to water dispensary sectors. In summary,  
294 considerable attention needs to be given to metakaolin-based geopolymer for water remediation, due to  
295 its purity, high surface area, in-built crystallinity and various kinds of metal oxides within its matrix

## 296 **5. Use of industrial waste as filler for the fabrication of crystalline metakaolin-based geopolymer.**

### 297 **5.1 Fly ash**

298 Fly ashes are fine and glassy powders that are recovered as a byproduct of coal combustion  
299 (used for production of electricity etc.). It consists of substantial amounts of silicon dioxide ( $\text{SiO}_2$ ),  
300 calcium oxide ( $\text{CaO}$ ), aluminum oxide ( $\text{Al}_2\text{O}_3$ ) and iron oxide ( $\text{Fe}_2\text{O}_3$ ) in Fig. 5 (Pacheco-Torgal et al.,

2008). Glassy particles (e.g. quartz, and mullite) are the major portions of the material (KIM, 2012). These make fly ash a good composite for the fabrication of geopolymer. Two classes (namely F and C) of this fly ash are particularly useful for geopolymer synthesis.

Class-F is produced mainly by burning harder, older anthracite and bituminous coal. Compositionally, this fly ash is pozzolanic in nature, and contains less than 7 % lime (CaO). Class-C fly ash is produced from the burning of younger lignite or sub-bituminous coal. In addition to pozzolanic properties; Class-C also has some self-cementing properties due to its CaO (i.e. lime) content (~20 %) (Ahmaruzzaman, 2010; KIM, 2012; Pacheco-Torgal et al., 2008). In fact, a Class-C fly ash requires lesser amount of alkaline activator when compared to class-F, for the geopolymer fabrication. In general, the use of fly-ash as a filler in geopolymers increases its compressive strength, surface area and catalytic sites. This in fact would be a viable means to use the fly ash derived from coal-powered stations. This offers a rather clean production of geopolymers in several countries (including China) that are strongly depended on coal-based electricity. This will be so, due to the fact that a high magnitude of fly-ash will be removed from environment, and of course, threat of heavy metals leaching from the fly-ashes (i.e. in the dumping sites) to water bodies is likely to be allayed. For instance, Motorwala et al. (2008) reported low-calcium fly ash (i.e. Class-F fly ash) for geopolymer synthesis. In their report, the following raw materials; coarse aggregate and fine aggregate sand, fly-ash, sodium silicate and different concentration of NaOH solution (i.e. 8M, 10M, and 12M) are used for the geopolymer production. Therein, all the constituents are thoroughly mixed together and cast into a cube to form concrete and left for 30 min under ambient condition before curing aging for 24 h at various temperature. The highest curing temperature gives the highest compressive strength with no further improvement after 80°C. Their work shows that the compressive strength of the geopolymer increases with an increase in the fly ash content; reverse is the case with an increase in extra water content. In addition to this, fly ash-based geopolymers do have the following physical properties: (i) the higher the alkaline concentration the better the compressive strength of geopolymer, (ii) the higher the ratio of sodium silicate solution-to-sodium hydroxide solution by mass, the higher is the compressive strength of geopolymer concrete.

327 All these show the significance of fly ash when it is being selected as component or filler for  
328 metakaolin-based geopolymers. This will eventually have direct advantages when such geopolymer  
329 composites are used for adsorption and stabilization of both heavy metals and hazardous organic  
330 molecules (Zhuang et al., 2016). Furthermore, considering the high contents of  $\text{Fe}_2\text{O}_3$  in fly ash (Yu et  
331 al., 2012), it is likely that using it either as a composite or single phase geopolymer material that will  
332 meet the requirements for real-world practical applications of photocatalysis.

333 In summary, nanoparticle impregnation in geopolymer matrices and in some cases elimination  
334 of the need for nanoparticle embedment is plausible for achieving desired catalytic activity  
335 enhancement. With this, low cost and eco-friendly geopolymer-based catalysts can be produced.  
336 Considering this, cleaner production is likely to be achieved in the field of complete water remediation,  
337 since excessive use of nanoparticle containing materials in water systems also has negative side-effects  
338 if not properly handled (Agarwal et al., 2013). Of course whether or not this will happen will depend  
339 upon the synthetic approaches that will be employed.

## 340 **5.2 Slag based geopolymer**

341 Slag is another interesting geopolymer filler for stability enhancement, and is commonly produced  
342 from industrial manufacturing processes like iron ore purification, and combustion of coke residue,  
343 limestone, and serpentine (Fhwa, 1998; Saheb, 2012). This material is sub-categorized into three types  
344 depending on the process of its formation as illustrated in Fig.6. For instance, blast furnace slag (BFS) is  
345 formed from iron, while both basic oxygen furnace slag (BOFS) and electric arc furnace slag (EAFS) are  
346 formed from steel (Proctor et al., 2000). Lime is the common chemical composition of all the three types  
347 of slag (Proctor et al., 2000). BFS is primarily made up of silica and alumina with various amounts of  
348 lime depending on the quantity of fluxing agent used in the iron or steel processing (McGannon, 1971).  
349 However, all three types of the slag are similar in composition except iron and manganese contents  
350 which are higher in BOFS and EAFS when compared to BFS (McGannon, 1971). Use of slag as an  
351 additive in the geopolymer fabrication may be of advantages (i.e. especially for the applications that  
352 involve catalysis and cleaned water reclamation). This is for the fact that the high content of  $\text{SiO}_2$  (~

353 30%) in BFS will increase workability and stability of the final geopolymer (Deb et al., 2014) which in  
354 turn will enable high pulverization of the materials into small particle sizes with uniform radius prior its  
355 use as catalysts or adsorbents. In fact, a substantial catalytic performance is likely to be achieved since a  
356 material with uniform surface or/and spherical shape enables ease with which water flow through it  
357 thereby bringing molecules into direct contact with the active sites. Furthermore, other advantages are  
358 likely to be achieved: (i) minimization of waste produced by iron and steel companies, (ii) reduction of  
359 the cost of production wherein BFS will serve as additional silica source thereby reducing the demand of  
360 the alkaline solution, (iii) high mechanical strength of geopolymer, offering lower maintenance and  
361 operation costs of metakaolin derived geopolymers, (iv) increase in the available land for the other uses  
362 (since slag storage requirements would reduce), and (v) minimization of the toxicity concerns around  
363 slag storage and management (since this is a known source of metal-containing leachates). It is evident  
364 that geopolymer production has several advantages from a cleaner production standpoint.

365 It worth here to say that all kinds of BFS serves pre-cleaner processes during the iron-smelting  
366 stages by trapping-out  $\text{SO}_2$  gas before being cooled and discharged into the environment. Nevertheless,  
367 BFS can be distinctly further sub-divided into different categories (i.e. foamed blast furnace slag,  
368 pelletized blast furnace slag, granulated blast furnace slag); depending on the method employed in the  
369 cooling of the final BFS. Although all forms of BFS are relevant; due to the presence of significant  
370 amounts of silica, aluminosilicates, and calcium-alumina-silicates in them, however granulated BFS  
371 seems more promising. This is because granulated BFS is made-up of small particles with high specific  
372 surface area, therefore making it an excellent candidate for the geopolymer fabrication (Robayo et al.,  
373 2016; Xu et al., 2014). Considering this fact, BFS-based geopolymer is likely thus to have high  
374 regeneration or recyclability after their initial deployment for water reclamation or photocatalysis. Table  
375 3 shows the chemical composition of granulated BFS, where a high content of calcium and silicon oxide  
376 are observable. The silicon in BFS often used to supplement the alkaline solution, making the  
377 geopolymerization process rapid and effective.

378 Nevertheless, prior to the deployment of these materials (i.e. both fly ash and BFS-based  
 379 geopolymer) for water reclamation and catalysis, a pre-analytical examination is considered paramount in  
 380 order to assess the heavy metal leaching rate of the systems. However, oftentimes these materials are  
 381 regarded as good binders with high density of binding sites for heavy metals within their matrices. The  
 382 mechanism involved in this process (i.e. entrapment of heavy metals within geopolymer matrix) is  
 383 related to the fact that the metal-ions often participate in the charge-balancing of  $[\text{AlO}_4]^{5-}$  in the  
 384 geopolymer network (Vu and Tran, 2018), thereby undergoing mechanical entrapment within the  
 385 geopolymer after solidification. For instance, Izquierdo et al. (2009) reported fly ash-slag based  
 386 geopolymer with microstructure surfaces; leaching rate of heavy metals from the synthesized  
 387 geopolymer is recorded. In their report, the fly ash-slag based geopolymer is synthesized without prior  
 388 thermal activation of starting materials.

389 **Table 3:** Chemical composition of BFS.(Emery, 1992)

Constituent	Percent
Calcium Oxide (CaO)	31-48
Silicon Dioxide (SiO <sub>2</sub> )	27-45
Aluminum Oxide (Al <sub>2</sub> O <sub>3</sub> )	7-18
Magnesium Oxide (MgO)	2-19
Iron (FeO or Fe <sub>2</sub> O <sub>3</sub> )	0.1-1.6
Manganese Oxide (MnO)	0.1-2.3
Sulfur (S)	1.0-2.3

390  
 391 The fly ash is mixed with the blast furnace slag, water and an activator solution ( $\text{SiO}_2/\text{K}_2\text{O} = 1.25$ ). The  
 392 geopolymeric paste obtained is then cast into cylindrical containers (diameter 29 and 39 mm height) and  
 393 cured in a closed container at room temperature for 28 days. The process generates geopolymer with a  
 394 desirable microstructure, and even with this, the batch leaching test performed on the sample shows that  
 395 fly ash-BFS based geopolymer inhibits metals mobility. Results prove that a number of trace pollutants  
 396 such as Ba, Be, Bi, Cd, Co, Cr, Cu, Nb, Ni, Pb, Rb, Sr, Sn, Th, U, Y, and Zr are retained within the  
 397 geopolymer matrix. Thus, this can be regarded as a cleaned product from a production process. In fact,  
 398 such remarkable result is attributed to mechanical strength resulting from good compactness contributed

399 by BFS. In another interesting report shown by Cheng and Chiu, (2003); metakaolin-BFS based  
400 geopolymer with high fire-resistance are obtained. In their report, granulated BFS is used as filler to  
401 increase mechanical strength and ability to withstand fire. The fire resistance property is conducted by  
402 subjecting the 10 mm thickness of the as-synthesized geopolymer into 1100°C flame; with the reverse-  
403 side temperature measurement reaches less than 240-283°C after 35 min. In summary, it is will be  
404 reasonable to say that slag can be used as reinforcement for crystalline metakaolin-, fly ash-based  
405 geopolymer to attain environmental stability after thermo- or photo-mechanical entrapment or conversion  
406 of either organic or inorganic hazardous substances. Other such novel controls and modifications on the  
407 mesoporous/crystalline geopolymers, are likely and will open avenues in near future for further adoption  
408 of this ceramic material in heavy metal adsorption, organic molecule photodegradation, radioactive  
409 encapsulation and micro-organisms disinfectants.

### 410 **5.3 BET surface area and pore structure correlation with synthesis applications.**

411 In catalytic applications and heavy metal adsorption, the performance of photocatalysts and  
412 adsorbents often progresses with certain structural properties (e.g. pore volume and surface area).  
413 Geopolymers are well known materials which often consist of high pore volume and large surface area.  
414 These have been found to substantially contribute to heavy metal adsorption. Synthesis methods play a  
415 significant role in fine-tuning these properties. For instance, Tang et al., (2015) reported a metakaolin  
416 based geopolymer with a BET surface area of 53.95 m<sup>2</sup>/g and porosity of about 60.30%. The high surface  
417 area and porosity are derived through the use of suspension and solidification method, where foaming  
418 agent SLS (i.e. K<sub>12</sub> sodium lauryl sulphate) is used to increase the mesoporous nature of the geopolymer.  
419 This geopolymer shows high adsorption capacity for Pb<sup>2+</sup>, Cu<sup>2+</sup> and Ca<sup>2+</sup> with removal capacity of 45.6,  
420 35.5 and 24.0 mg/g respectively. Spherically shaped geopolymer/alginate hybrid with high BET surface  
421 area (16.2 m<sup>2</sup>/g), pore size (11.5 nm) and pore volume of 0.05 mL/g is also reported by Ge et al., (2017)  
422 via one-pot impregnation method. In fact, this specific surface area (i.e. 16.2 m<sup>2</sup>/g) is about 1.7 times  
423 higher than of pure metakaolin-based geopolymer (i.e. with BET surface area of ~9.6 m<sup>2</sup>/g) (Ge et al.,  
424 2017). The use of sodium alginate to coat the metakaolin based geopolymer in an CaCl<sub>2</sub> aqueous solution

425 is known to be an efficient method to create mesoporous surface and abundant inner pores which  
426 contribute immensely to the high adsorption capacity towards Cu(II) (Ge et al., 2017). Similarly, Lee et  
427 al. (2016) have recently shown that post-hydrothermal treatment method can be used to obtain fly-ash  
428 based geopolymer with high surface area and pore volume of 114.16 m<sup>2</sup>/g and 0.2677 cm<sup>3</sup>/g respectively.  
429 These obviously give advantages such as high adsorption capacity relevant for the removal of Cs<sup>+</sup> from  
430 aqueous solution (Lee et al., 2017). Hence synthesis methods continue to be relevant for improving the  
431 surface area and pore volume of the geopolymers for water remediation and related applications.

## 432 **6. Result and Discussion on applications driven by the surface chemistry of geopolymers in water**

433 Geopolymer surfaces tend to have photoactive sites, due to the presence of metal oxide moieties.  
434 This makes it directly relevant for disinfection. Also given its porosity, the phases that are not  
435 photoactive could find application as adsorbents. In particular, heavy metal ion adsorption has been most  
436 widely explored (Siyal et al., 2018).

437 Despite all of the above; geopolymers, do not compete favorably with nanoparticles with respect  
438 to catalytic and adsorptive applications (Falah, 2015). However, efforts to improve the catalytic and  
439 adsorptive functionalities would be valuable since geopolymers offer obvious advantages (primarily  
440 scalable, and cleaner production from fly ash and metakaolin composites is obviously favorable for  
441 photocatalysis, and the presence of crystalline metakaolin favors heavy metal adsorption) (Xu and  
442 Deventer, 2000; Zhang and Liu, 2013).

### 443 **6.1 Heavy metal adsorption by geopolymer**

444 Adsorption involves removal of metal ions using solid surfaces. Adhesion forces are created  
445 between the metal ions and mesopores (reference to geopolymer is shown Fig.7) which is the reason for  
446 the observed adsorption. Mesoporous surfaces are also essential for desorption processes relevant for the  
447 regeneration/reusability of the adsorbents. This oftentimes is carried out through simple washing,  
448 chemical treatment, steam washing or thermal treatment. The adsorption process is either chemisorption

449 or physisorption depending on whether or not the adsorption results in the formation of a chemical bond.  
450 Oftentimes, physisorption adsorption process gives favorable adsorption and offers easy regeneration  
451 due to the weak Van der Waal interactions involved (ref: Fig. 7). In fact, this mechanism (i.e.  
452 physisorption adsorption process) gives high regeneration ability to the adsorbent with about  $\leq 1-10\%$   
453 reduction in the adsorption capacity for about 6-10 consecutive times of usage (Lata et al., 2015).  
454 Considering all the above pointers and its porosity, metakaolin-based geopolymer is likely to fulfill all  
455 the promising properties for adsorption operation. For instance, Cheng et al. (2012) have investigated the  
456 adsorption of four different heavy metals by using metakaolin-based geopolymers. The geopolymer is  
457 made by condensing the mixture of metakaolin and (NaOH) alkaline solution at room temperature, and  
458 the geopolymer is pre-crushed to a fixed-radius size through the use of sieving devices. The geopolymer  
459 exhibits excellent adsorption capacity towards (i.e.  $Pb^{2+}$ ,  $Cu^{2+}$ ,  $Cr^{3+}$ , and  $Cd^{2+}$ ) due to its high porosity  
460 and surface area. This outstanding performance of  $\sim 90\%$  removal capacity towards all the metal ions is  
461 related to the mesoporous surface created by Al-Si-O network. In another interesting report given by  
462 López et al. (2014), metakaolin-based geopolymer is used as a selective adsorbent; it is prepared from a  
463 mixture of silica and metakaolin, and applied for the selective removal of  $Cs^+$  and  $Pb^{2+}$  from heavy metal  
464 ions mixture. The heavy metal adsorption behavior is described well using the Langmuir model, which  
465 proves that the metakaolin-based geopolymer has multiple and different types of binding active sites;  
466 this is attributed to the formation of more than one adsorptive layer (i.e. for  $Cs^+$  and  $Pb^{2+}$ ). Similarly, Al-  
467 Zboon et al. (2016) reported natural volcanic tuff based geopolymer for the removal of  $Zn^{2+}$  with the  
468 efficient uptake of 97.7 % against 78.5 % of ordinary/natural volcanic tuff (porous rock formed by  
469 volcanic ash consolidation) as it is previously reported. In their research work, batch adsorption  
470 technique is used to study the adsorption isotherms of  $Zn^{2+}$  onto the geopolymer surface. Different  
471 concentrations of  $Zn^{2+}$  are added to a constant dose of geopolymer (0.4 g) at different temperatures (25,  
472 35, 45 °C) and at different pH values (5, 6, and 7). The removal efficiency increases as the geopolymer  
473 dosage, contact time and temperature increases. This implies that the adsorption active sites of the  
474 geopolymer do not get saturated instantly, and a gradual increase in the metal-ion transfer onto the

475 surface of the geopolymer is observed up to the point where the equilibrium position is established. This  
476 is due to the high density of adsorptive sites present in the geopolymers, which are not gotten saturated  
477 instantaneously. Thus, this shows that metakaolin-based geopolymers can serve as wastewater purifier in  
478 a bed filter systems (i.e. heavy metal getters) for a real world applications. In addition to this, use of  
479 metakaolin-based geopolymer for the fabrication and design of water pipe-lines is likely to bring low-  
480 cost water circulation in both urban and rural areas for the fact that the materials are from the geological  
481 origins, and the threats of trace and heavy metals can be well prevented with this system. Naghsh and  
482 Shams, (2017) recently used kaolin based geopolymer for efficient removal of  $\text{Ca}^{2+}$  and  $\text{Mg}^{2+}$  from  
483 aqueous solution. It is however shown that the high charge density and easy hydration of the  $\text{Mg}^{2+}$  (Siyal  
484 et al., 2018) usually results in ready precipitation, which in turn causes lower removal rates when  
485 compared to  $\text{Ca}^{2+}$ . In case of  $\text{Ca}^{2+}$ , the larger ionic size radius (i.e. ionic size radius of  $\text{Ca}^{2+}=0.99\text{\AA}$  and  
486  $\text{Mg}^{2+}=0.66\text{\AA}$ ) makes it rather readily removable using geopolymer adsorbents. In fact,  $\text{Ca}^{2+}$  is likely to  
487 have higher transfer rates toward the pores and adsorptive sites of the geopolymer (Tognonvi et al.,  
488 2012). Due to the ability to remove  $\text{Ca}^{2+}$ , geopolymers are promising softeners for elimination of water  
489 hardness making it a promising material for the cleaner production of laundry houses and alike.

490 Not only metakaolin-based geopolymers; but also fly-ash-based geopolymer has been proven to be a  
491 good adsorbents for heavy metals, (Al-Harashsheh et al., 2015). In fact, the presence of several metal  
492 oxides phases (e.g.  $\text{Fe}_2\text{O}_3$ ,  $\text{SiO}_2$  and  $\text{Al}_2\text{O}_3$ ) (Al-Zboon et al., 2011), in this system plays an important  
493 role since it contributes to the enhancement of specific surface area (with a contribution of as high as  
494  $\sim 74.6\%$  pore volume) (Duan et al., 2016). In fact, in order to form fine particles and to achieve enough  
495 mesoporous surface on crystalline metakaolin-based geopolymer; surface modification with fly ash is  
496 likely to be a way out. Further advantage can be obtained by employing high density anionic ends ( $\text{O}^{2-}$ )  
497 in such a composite system which will ensure rapid getting of metal ions through ionic exchange  
498 processes. Furthermore, the well exposed oxygen atoms in the geopolymer matrix will facilitate  
499 formation of heavy metals- $\text{O}_2$  complexes, and hence will result in precipitates from the water solution.

500 This will lead to substantial removal of the toxic metal-ions from water. Table 4 shows various  
 501 geopolymeric adsorbents used for the removal of heavy metal-ions from aqueous solution. Therein, most  
 502 of the results fitted well into Langmuir isotherm, this indicates chemisorptive adsorption process (Batool  
 503 et al., 2018), as a result of bond interaction between the anionic ends (i.e. adsorbent sites) and the metal  
 504 ions.

505 **Table 4:** Various work done on the adsorption of heavy metals onto geopolymer adsorbent.

Adsorbent	medium	Removal capacity	Model	Heavy metal	Ref.
FA based G	WW	152mg/g	L, Ho	Cu <sup>2+</sup>	(Al-Harashseh et al., 2015)
ZT based G	AS	7.8mg/g	-	Cu <sup>2+</sup>	(Alshaaer et al., 2015)
FA based G	AS	97.7%	L	Pb <sup>2+</sup>	(Al-Zboon et al., 2011)
NVT based G	AS	100%	L	Zn <sup>2+</sup>	(Al-Zboon et al., 2016)
MK based G	AS	100%	L	Zn <sup>2+</sup> , Cu <sup>2+</sup> , Cd <sup>2+</sup>	(Andrejkovičová et al., 2016)
MK based G	AS	-	L	Sr <sup>2+</sup> , Co <sup>2+</sup> , Cs <sup>+</sup>	(Chen et al., 2013)
MK based G	AS	-	L, Ho	Pb <sup>2+</sup> , Cu <sup>2+</sup> , Cr <sup>3+</sup>	(Cheng et al., 2012)
FA based G	WW	113.41mg/g	F, L	Cu <sup>2+</sup>	(Duan et al., 2016)
MK based G	WW	-	-	Ni <sup>2+</sup>	(Ge et al., 2015b)
MK based G	AS	-	L, Ho	Cu <sup>2+</sup>	(Ge et al., 2015a)
PA based G	AS	99±3.4%	L, Ho	Cu <sup>2+</sup>	(Ge et al., 2017)
Z based G	AS	-	L, Ho	Cu <sup>2+</sup>	(Javadian et al., 2015)
MK based G	AS	-	L, Ho	Zn <sup>2+</sup> , Ni <sup>2+</sup>	(Kara et al., 2017)
FA based G	AS	118.6mg/g	Ho	Pb <sup>2+</sup>	(Liu et al., 2016)
MK based G	AS	-	-	Cs <sup>+</sup>	(Luukkonen et al., 2016)
BFS based G	SME	90-100%	L,F,	Ni <sup>2+</sup> , AS <sup>2+</sup> , Sb <sup>2+</sup>	(Luukkonen et al., 2016)
FA based G	WW	-	Ho	Cu <sup>2+</sup>	(Mužek et al., 2014)
FA based G	AS	6.34mg/g	-	Pb <sup>2+</sup>	(Novais et al., 2016)
BFS based G	WW	85.29mg/g	L, Ho	Ni <sup>2+</sup>	(Sarkar et al., 2017)

506 Note; \*L: Langmuir isotherm, \*F: Freundlich isotherm, \*BFS: blast furnace slag, \*FA: fly Ash, \*MK:  
 507 metakaolin, \*Z: zeolite, \*ZT: zeolitic tuff, \*NVT: natural volcanic tuff, \*PA: polymer-alginate, \*G:  
 508 geopolymer, H<sub>o</sub>: pseudo-second-order, WW: wastewater, AS: aqueous solution, \*SME: spike mine  
 509 effluent.

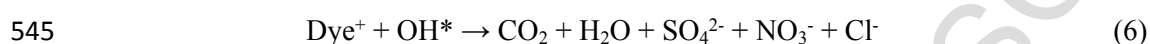
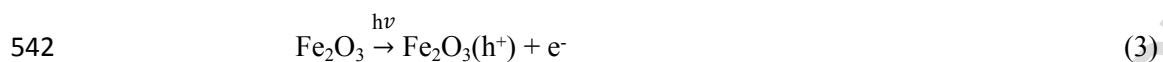
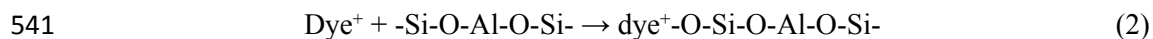
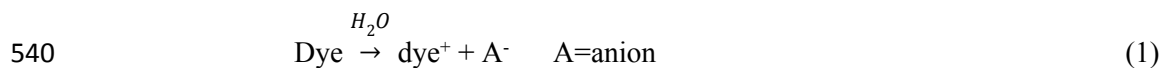
510 Pseudo-first and pseudo-second-order, and intra-particle diffusion models consist of kinetic  
 511 parameters often used to investigate thermo-chemical adsorption process fully detailed elsewhere (El-  
 512 Geundi, 1991; Itodo et al., 2010). Fly-ash/metakaolin-based geopolymers often show remarkable  
 513 adsorption capacity towards divalent metal ions (e.g. Pb<sup>2+</sup>, Cu<sup>2+</sup>, Sr<sup>2+</sup>, Co<sup>2+</sup>, Cs<sup>+</sup>, Cu<sup>2+</sup> Cd<sup>2+</sup>, Zn<sup>2+</sup>, Ni<sup>2+</sup>),

514 as demonstrated (Cheng et al., 2012; Ge et al., 2015a; Kara et al., 2017), with pseudo-second-order  
515 adsorption process, which in turn indicates that the heterogeneous surface of the geopolymers are  
516 favorable for the removal of the metal ions.

517 In summary, fly-ash/metakaolin-based geopolymers which have metal oxide inclusions and which  
518 are composites with large surface areas offer advantages that can be further leveraged for the  
519 development of cheap adsorbents for heavy metal removal from contaminated water.

## 520 **6.2 Catalyst derived geopolymer.**

521 Due to the resistance of most organic molecules (e.g. dyes,  $\text{Cl}^-$  and  $\text{NO}_x$  containing molecules) to the  
522 mineralization, a catalyst is often employed for hastening their degradation. In fact, since  
523 photodegradation rather than traditional adsorption process is considered as the efficient way to  
524 completely remove hazardous organic molecules from water, it is reasonable to dwell on this theme.  
525 Recently geopolymers have been explored as co-catalyst or/and as supports for photocatalytic degradation  
526 of these organic compounds. Owing to its high surface area, porosity, and photoactivity, these nano-metal  
527 oxides (e.g.  $\text{Fe}_2\text{O}_3$ ) (ref: Fig.8) offer rapid initial adsorption of the target organic molecules (Rui et al.,  
528 2018; Zhang et al., 2015). This is followed by subsequent oxidative/hydrolytic reaction (Kovářík et al.,  
529 2017; Novais et al., 2018). Particularly, fly-ash based geopolymer has been used to achieve ~92.7%  
530 photodegradation of methylene blue (MB) under UV irradiation (Zhang and Liu, 2013). The observed  
531 desirable performance is attributed to presence of several pores (mostly in the range ~17– 700 nm) and  
532 semiconductor metal oxides present in the geopolymers. The simple photocatalytic mechanism is carried  
533 out by metal oxides in these geopolymers. The process is enabled by the ionization of MB dye molecules  
534 to a cation (reaction 1), which is followed by the adsorption of the cation onto negatively charged  
535 tetrahedron  $[\text{AlO}_4]^{5-}$  (reaction 2). Thereafter, the photo-excitation of the semiconductor  $\text{Fe}_2\text{O}_3$  in the  
536 geopolymer leads to the formation of an electron ( $e^-$ ) - hole ( $h^+$ ) pair (reaction 3). Consequently, the  
537 reduction of  $\text{Fe}^{3+}$  to  $\text{Fe}^{2+}$  in the fly ash-based geopolymer ensures rapid hydrolytic reaction between the  
538 hole ( $h^+$ ) and  $\text{H}_2\text{O}$  molecule to produce hydroxyl radical (reaction 5). This subsequently results in the  
539 mineralization of the cationic methylene blue (reaction 6) (Zhang and Liu, 2013).



546 The interesting fact about this ceramic-photocatalyst is that various kinds of metal oxides (e.g.  
 547  $\text{Fe}_2\text{O}_3$ ,  $\text{TiO}_2$ ,  $\text{Al}_2\text{O}_3$ , and  $\text{MgO}$ ) are formed in the Al-O-Si-O- framework during geopolymerization.  
 548 These are photocatalysts useful for degradation of organic molecules. In fact such catalytic reaction is  
 549 likely to be achieved under visible light irradiation provided surface functionalization and tailoring are  
 550 employed (Falah et al., 2016; Falah, 2015).

551 From literature conducted so far, the high pore volume of metakaolin-based geopolymer is utilized  
 552 to incorporate  $\text{TiO}_2$ , so as to obtain  $\text{TiO}_2$ -nanoparticles-geopolymer composites (Ancora et al., 2012).  
 553 The geopolymer matrix exhibits excellent catalytic activities not only at the surface, as is often reported;  
 554 but also in the bulk of the composite (due to sufficient porosity). Similarly, thin film titanium oxide  
 555 ( $\text{TiO}_2$ ) nanoparticle is coated on the surface of geopolymer for photocatalytic degradation of methylene  
 556 blue (Chen et al., 2017). Such systems exhibit high activity which can be attributed to the combination  
 557 of high porosity and overall pore volume (i.e. surface area of  $216 \text{ m}^2 \text{ g}^{-1}$  and pore volume of  $0.22 \text{ cm}^3 \text{ g}^{-1}$ )  
 558 <sup>1)</sup> (Singhal et al., 2017). Considering the high toxicity of these dyes coupled with the threats they cause  
 559 to water bodies; complete mineralization can indeed be considered as a cleaner-approach rather than  
 560 mere adsorption (which is so often reported). In another interesting report, both  $\text{TiO}_2$  and  $\text{Cu}_2\text{O}$   
 561 nanoparticles are used to modify catalytic properties of metakaolin-based geopolymer (Falah et al.,  
 562 2016). The two metal oxides are used to increase the density of cations in the system (ref: Fig. 9) as the

563 catalytic active sites.

564 A recent report by Falah et al. (2016) is notable in the above context; here precipitation of metal  
565 oxides beneath fly ash-based geopolymer (FAG) during photocatalytic activity is investigated by varying  
566 pH of reaction medium (i.e. aqueous solution). Therein, it is highlighted that pH fluctuation affects the  
567 photocatalytic activities owing to in situ metal oxides precipitation. This in turn results in the formation of  
568 hydroxides on the surface and pores of the geopolymer. Interestingly, this is rather effectively solved by  
569 Falah et al. (2016) using cetyltrimethylammonium bromide (CTAB) which hinders the precipitation  
570 process. In fact used of CTAB increases the pH tolerance of the modified geopolymer as well as its  
571 photocatalytic performances. Thus, the use of surfactant or reductants (such as poly(vinyl alcohol), citric,  
572 tartaric acid, gluconic acid, hydroxamate, dimercaptosuccinic acid, or phosphoryl choline) to control the  
573 size and shape of the prominent metal oxides (e.g.  $\text{Fe}_2\text{O}_3$ ) is likely to make the system suitable for  
574 advanced catalysis. In fact, nanostructure properties can be achieved through this approach since use of  
575 surfactant is considered as a way of tailoring material surfaces, particles sizes, morphologies, surface  
576 areas and intra-particle ionic strengths. This can also be done through pH-adjustment (Stojanovic et al.,  
577 2018).

578 Furthermore, graphene is used to dramatically improve the conductivity of fly-ash/graphene-based  
579 geopolymer (FAG) (Zhang et al., 2018), where graphene serves as electron acceptor to improve electronic  
580 conductivity of geopolymer (i.e. ~348.8times increase in electronic conductivity, as shown in Fig. 10a),  
581 this consequently gives rise to a significant photodegradation of indigo carmine dye through the  
582 photogenerated hydroxyl radical under UV irradiation (Fig 10b-c). In fact, the system exhibits appreciable  
583 regeneration ability with activity retention of ~90 % over 5times of recyclability (Fig. 10d). Therefore, at  
584 present, it is reasonable to believe that surface modification of these materials (i.e. geopolymers) is  
585 helpful for catalytic applications. Nevertheless, there is certainly further scope for exploring experimental  
586 control in synthetic reactions; especially those that may lead to phase modification or/and incorporate  
587 crystal/nanostructures entities into geopolymer for better catalytic activity. For instance, a notable results

588 is one wherein alkali-activated granulated blast furnace slag-based geopolymer (BFSG) with a particle  
589 size in the range of ~50 nm (ref: Fig 11a) is synthesized via geopolymerization, and Fe<sub>2</sub>O<sub>3</sub> is incorporated  
590 into the system using impregnation methods (Yao et al., 2013). Significant photocatalytic degradation of  
591 Congo Red (CR) dye is observed (ref: Fig. 11b-c), for reasons mainly attributed to the prohibition of  
592 recombination of photogenerated hole-electron (Fig. 11d). In fact, here it is important to note that BFS-  
593 based geopolymer enables substitution of Fe<sup>3+</sup> (i.e. of Fe<sub>2</sub>O<sub>3</sub> nanoparticles) with Na<sup>+</sup>, Al<sup>3+</sup> and Ca<sup>2+</sup>  
594 (Sazama et al., 2011; Zhang et al., 2012); this is known to increase the photo-activity substantially.

595 Ionic exchange mechanism like the ones depicted in Fig. 12 has been used by Zhang et al. (2012) for  
596 the fabrication of nickel-alkali-activated steel slag-based geopolymer, where Ni<sup>2+</sup> is used to replace  
597 almost all the Na<sup>+</sup> ions in the matrix of (Na, Ca)-cementitious geopolymer. The ionic replacement ensures  
598 reduction of electronic conductivity resistance (i.e. a UV-vis and near infrared ray spectrum undergoes  
599 blue shift), due to the strong interaction between Ni<sup>2+</sup> and negative charge of [AlO<sub>4</sub>]<sup>5-</sup> tetrahedron in the  
600 framework of the geopolymer material. The host ([AlO<sub>4</sub>]<sup>5-</sup>) and guest (Ni<sup>2+</sup>) undergo interaction, that  
601 often involves Van der Waal forces (ref: Fig. 12) (Li et al., 2016), which eventually favors fast electron  
602 excitation to conduction bands.

603 Considering the reasonable compatibility of metal oxides/metallic nanoparticles or graphene with  
604 geopolymers for photocatalytic activity; the aggregate forms of the Mn<sup>2+</sup>, CuO and graphene has been  
605 used recently to functionalize alkali-activated geopolymer for both catalytic hydrogen evolution and  
606 direct sky blue 5B dye degradation (Zhang et al., 2017). In fact, due to uniform distribution of all the  
607 guests in the mesoporous structure of the geopolymer (with small crystallite sizes and good electronic  
608 couplings) (ref: Fig. 13a, inset shows the composition distribution), about 2853.7 mmol g<sup>-1</sup> of hydrogen is  
609 successfully generated (ref: Fig. 13b), making the system relevant for catalytic purposes in energy  
610 production. Likewise with this system ~100% photodegradation of direct sky blue 5B dye (Fig. 13c) is  
611 achieved under visible light irradiation. Hence a plausible cleaner production approach (e.g. involving  
612 water splitting-oxygen evolution and hydrogen evolution reaction) can be envisaged if good electron

613 conductors like metal nitrides and carbides are used for surface functionalization of the geopolymer.  
614 However, further investigation is recommended to examine the exact mechanism involved in the process  
615 of surface functionalization. This will enable reasonable identification and quantification of the catalytic  
616 active sites in these materials.

617 In summary, given the above discussion, it is clear that geopolymer composites are promising  
618 catalyst supports. However if the pure phase of the geopolymer is to be employed for photocatalysis or  
619 electrocatalysis in future, surface tailoring and experimental controls (i.e. use of surfactant to improve pH  
620 tolerances and specific surface areas) is likely to be a way forward. Furthermore, nanostructuring of  
621 geopolymers could also offer a means to enhance its photoactivity an eventual utility.

### 622 **6.3 Antibacterial derived geopolymer**

623 Geopolymer is being considered as functional-surface-coating materials for inhibiting the growth of  
624 bacteria (Bortnovsky et al., 2010; Moya et al., 2013). This system is often used to change the surface  
625 properties of the substrate in order to make it tolerant to the wetter and coastal organisms (e.g. planktons).  
626 For instances, in 2017, Pratama, (2017) synthesized nano-silver (Ag)-geopolymer composite as a  
627 functional surface coating material for bacteria growth inhibition. The Ag-nanoparticles is successfully  
628 incorporated onto the surface of geopolymer matrix via bioreduction mechanism. This process results in  
629 the need for a rather prolonged curing period; however after reaching a stable state, the function of each  
630 of the constituents is rather distinct. Nano-Ag and geopolymer matrix are considered as antibacterial and  
631 supportive refractory agents respectively. Before then, solution treatment method is applied for printing of  
632 copper chloride onto the surface metakaolin-based geopolymer (Hashimoto et al., 2015). Here,  
633 geopolymer matrix prepared from a mixture of metakaolin and potassium hydroxide (KOH) after 7days of  
634 curing (at temperature=60°C), is completely immersed in a solution of 0.1 mol/L  $\text{CuCl}_2$  for 24 h. This  
635 solid-state geopolymer changes from yellow to green due to ionic exchange. The system is then applied as  
636 antibacterial material; the desirable performance here is attributed to the mesoporous surface of the  
637 geopolymer which in turn enables fast and quick ionic exchange between the  $\text{Cu}^{2+}$  of  $\text{CuCl}_2$  and  $\text{K}^+$  of

638 geopolymer matrix. In fact, this approach can be used to solve the problem of prolonged curing time (akin  
639 to the bioreduction of  $\text{AgNO}_3$ ). This in fact allows easy scalability of the geopolymers as antibacterial  
640 materials/surfaces for the treatment of water containing micro-organisms. With this, different treatment  
641 measures for industrial wastewater (i.e. microbial, heavy metals and organic compounds removal) are  
642 likely to be achieved within a single geopolymer treatment plant. It will eventually reduce industrial  
643 production cost and enable industries to comply with environmental law and regulation.

644 In addition, geopolymers composites based on metakaolin and nano-ZnO for antibacterial  
645 applications are reported by Nur et al. (2017). Therein, a solid solution of metakaolin and ZnO-  
646 nanoparticles is made; this is then mixed with an alkaline solution (NaOH) to produce the geopolymer  
647 matrix. This system exhibits high mechanical strength, and is used to inhibit bacterial growth. Although,  
648 the nanoparticles can stand alone be a reasonable antibacterial; better performances are observed with  
649 ZnO-geopolymer composites (indicating co-activity from the matrix as well). Such activity can be  
650 attributed to the presence of a significant amount of metal oxides and Al-O-Si network in the geopolymer  
651 which plausibly offers synergistic anti-bacterial activity.

652 Likewise Triclosan-geopolymer composites have been reported as antibacterial agents against  
653 *Escherichia Coli* (Gram-negative bacteria) (Fig. 14a) and *Staphylococcus Aureus* (Gram-positive  
654 bacteria) (Fig, 14b) using the Halo method (Rubio-Avalos, 2018). The reproduction rate of these bacteria  
655 is effectively controlled through a substantial distribution of Triclosan in the geopolymer substrate that  
656 serves as reinforcement and disperser. However, use of nanoparticles in composite forms to functionalize  
657 the surface of geopolymer for inhibiting the growth of sulphuroxidizing microbes and other alkaline-  
658 tolerant microbes, (i.e. colony at the surface of concrete) is considered as one of best systems (Diercks et  
659 al., 1991; Islander et al., 1991; Wei et al., 2010). For instance, ZnO-SiO<sub>2</sub> composite coated fly ash-based  
660 geopolymer ( $\text{GM}_{\text{ZnO-Si}}$ ) (Sarkar et al., 2018), is used as an anti-microbial (i.e. against *E. coli*, *S. aureus*, *A.*  
661 *niger*) as shown in Fig. 15a-c, while maintaining the mechanical properties of the  $\text{GM}_{\text{ZnO-Si}}$  composite,  
662 therein the presence of the two nanoparticles phases (i.e. ZnO and SiO<sub>2</sub>) on the geopolymer make it

663 exhibits substantial antibacterial performances far better than the single nanoparticles ( $\text{SiO}_2$ ). Such  
664 performance indicates that high charge transfer from ZnO- $\text{SiO}_2$  hybrid within the geopolymer results in  
665 faster rupture of bacterial DNA when compared to the use of single phase  $\text{SiO}_2$  or ZnO (Sarkar et al.,  
666 2018).

667 In summary, antibacterial geopolymers are promising devices for the fabrication of water treatment  
668 plant, and water filter bed. In fact, they have potential to offer cleaner production routes for industrial,  
669 health and governmental sectors. However, overcoming challenges associated with incorporation of  
670 metal/metal oxides molecules onto the earthly abundant metakaolin is needed. This will have a bearing on  
671 tackling issues concerning scalability and stability. Furthermore, fly-ash/metakaolin-based geopolymer is  
672 likely to fill the space of metal oxides-nanoparticles/geopolymer composites as antibiotics in the near  
673 future. These possibilities are currently hindered by challenges highlighted below making geopolymer  
674 production in a scalable manner difficult, in practice.

## 675 **7. Barriers to utilization**

676 Currently, a number of technical and legal barriers are restricting the use of most waste materials (e.g.  
677 fly ash, and blast furnace slag) for any further application without prior treatment (Ahmaruzzaman,  
678 2010). This makes access to the industrial waste materials rather difficult, which in turn causes limited  
679 research work on them. The major constraints are the lack of data related to their specifications, in-  
680 process standardization, and characterization data from the production centers. However, proper  
681 institutional documentation and specification is likely to remove most of these barriers.

682 Likewise logistic barriers exist due to the bulky nature of the precursors (i.e. BFS, kaolin, fly ash) which  
683 makes their transportation difficult. Allocation of reasonable funds from both institutes, non- and  
684 governmental sectors are likely to further increase the interest of research communities in the design and  
685 fabrication of advanced geopolymer-based catalysts for cleaner production (especially for applications  
686 related to water remediation).

687 Another obvious barrier is the legal restriction placed on the exploitation of natural minerals like kaolin  
688 in many countries and regions (e.g. ref: Minnesota's Mining Laws in states) making the raw materials  
689 expensive, which in turn limits their applications. Application of geopolymer for the removal of  
690 hazardous heavy metals and organic compounds is an efficient and effective approach. However,  
691 regeneration of the spent geopolymeric-photocatalyst and/or adsorbent by backwashing with water is  
692 still a challenge and never reported so far. Although for other materials like nanoparticles and activated  
693 charcoal, just to mention few; different regeneration methods (e.g. chemical treatment, backwashing,  
694 thermal treatment, and steam treatment) have been reported for the treatment of the spent  
695 adsorbent/photocatalysts (Burakov et al., 2017; Lata et al., 2015; Rasaki et al., 2018). Among these  
696 methods, thermal treatment, back- and steam-washing seem effective. Chemical treatment too appear to  
697 be a promising method for geopolymer (Naghsh and Shams, 2017). Furthermore safe disposal of the  
698 materials after using them into a geotextile landfill is crucial (Richardson and Zhao, 2010; Rowe, 2007).  
699 Reduction in the compressive strength and stability after incorporating metal oxides/nanoparticles into  
700 the geopolymer matrix often hinders the crushing and pulverization of the solid geopolymers; this is  
701 another great challenge.

## 702 **8. Future research and prospects**

703 Geopolymers offer substantial prospective value in environmental remediation technologies. Its  
704 high flexural strength, low carbon footprint, fast curing time and solidification, high fire and poison  
705 resistance, offer fresh possibilities for researchers. When engineered, it has the potential to perform even  
706 better than activated carbon or zeolites for the adsorption of hazardous materials both in the air or water  
707 polluted environment. This is due to its high porosity. Adsorption performance of geopolymer depends  
708 on raw materials used for its synthesis. With appropriate use of precursors and synthetic strategies, waste  
709 water can be easily converted to cleaned water through use of geopolymer as a purifier.

710 Furthermore, geopolymers can be viable photocatalyst supports, due to its characteristic  
711 composition which yield various metal oxides. However, further research is required in provision of  
712 scalable technologies involving geopolymers adsorbent and photocatalyst supports. Surface

713 nanostructuring, coating and composites generation are likely to be major activities to this end, in near  
714 future. Synthesis and process controls will be relevant to optimize in all these cases.

## 715 **9. Conclusion**

716 Geopolymeric materials can offer valuable solutions to environmental remediation challenges.  
717 These solutions are likely to be low on infrastructure maintenance, and of relevance to the scalability  
718 needs of current industrial waste water treatment plants. The possibility of (i) synthesizing from  
719 accessible and rather abundantly available raw materials and (ii) fabrication using room temperature  
720 approaches with low or zero green house gases emission have made geopolymer a material relevant for  
721 cleaner production and for green technologies. This also offers windows of ‘green technology’  
722 opportunities in allied industries - including construction, surface engineering, and healthcare. Advanced  
723 uses of this material for catalysis applications and energy production will particularly benefit industries  
724 which focus on waste treatment and water remediation. We believe that this review will offer insights  
725 into the use of geopolymers as a plausibly green and sustainable material that offers viable solutions to  
726 global environmental challenges associated with waste water treatment, energy production and slag  
727 management. Furthermore the barriers to technology outlined in this work are expected to be of direct  
728 relevance to stakeholders of the various clean and green production sectors, and for policy makers in the  
729 government.

## 730 **Acknowledgement**

731 This work is supported by NSF China through grant 21471147, 2014020087 Liaoning, and National Key  
732 Research and Development Program of China through grant 2016YFB0101200, 2016YFB01012. M.  
733 Yang would like to thank for the National “Thousand Youth Talents” program of china and Ningbo  
734 3315 program. Tiju Thomas thanks the Indian Institute of Technology Madras and the Department of  
735 Science and Technology (DST, Government of India) for financial support in the form of grants  
736 including DST 01117 (INSPIRE), Young Scientist Scheme (YSS/2015/001712) and Centre grant  
737 CHY1718383DSTXTPRA (where he is a Center member). Tiju Thomas also thanks Ministry of  
738 Electronics & Information Technology for support Centre grant ELE1819353MEITENAK (wherein he

739 is Center member). He would also like to thank DST for support via Indian Solar Energy Harnessing  
 740 Center (ISEHC) – an Energy Consortium (DST/TMD/SERI/HUB/1(C)), wherein he is a inter-domain  
 741 coordinator. We thank all the relevant publishers (Elsevier, and Springer Nature) who granted us  
 742 copyright permissions for use of their printed works for this academic review article. The permits carry  
 743 the following IDs: 4417530291483, 4417021456321, 4417550183552, 4418091238497,  
 744 4417950347231, 4417020576404, 4416440368469, 4416430671904, 4416410493723, and  
 745 4416390107905 and will be available with the authors.

## 746 References

- 747 Abdul Rahim R.H., Rahmiati T., Azizli K.A., Man Z., Nuruddin M.F., Ismail L. (2014) Comparison of  
 748 Using NaOH and KOH Activated Fly Ash-Based Geopolymer on the Mechanical Properties.  
 749 *Materials Science Forum* 803:179-184.
- 750 Agarwal M., Murugan M.S., Sharma A., Rai R., Kamboj A., Sharma H., Roy S.K. (2013) Nanoparticles  
 751 and its toxic effects: A Review. *Int.J.Curr.Microbiol.App.Sci* 2(10): 76-82
- 752 Ahmaruzzaman M. (2010) A review on the utilization of fly ash. *Progress in Energy and Combustion*  
 753 *Science* 36:327-363. DOI: <https://doi.org/10.1016/j.pecs.2009.11.003>.
- 754 Aizat A. E., Abdullah M.M.A.B., Ming L., Yong H., Kamarudin H., A Aziz I. (2015) Review of  
 755 Geopolymer Materials for Thermal Insulating Applications.
- 756 Al-Harashsheh M.S., Al Zboon K., Al-Makhadmeh L., Hararah M., Mahasneh M. (2015) Fly ash based  
 757 geopolymer for heavy metal removal: A case study on copper removal. *Journal of Environmental*  
 758 *Chemical Engineering* 3:1669-1677.
- 759 Al-Zboon K., Al-Harashsheh M.S., Hani F.B. (2011) Fly ash-based geopolymer for Pb removal from  
 760 aqueous solution. *Journal of hazardous materials* 188:414-421.
- 761 Al-Zboon K.K., Al-smadi B.M., Al-Khawaldh S. (2016) Natural volcanic tuff-based geopolymer for Zn  
 762 removal: adsorption isotherm, kinetic, and thermodynamic study. *Water, Air, & Soil Pollution*  
 763 227:1-22.
- 764 Alshaaer M. (2013) Two-phase geopolymerization of kaolinite-based geopolymers. *Applied Clay Science*  
 765 86:162-168.
- 766 Alshaaer M., Mallouh S.A., Al-Kafawein J.a., Al-Faiyz Y., Fahmy T., Kallel A., Rocha F. (2017)  
 767 Fabrication, microstructural and mechanical characterization of Luffa Cylindrical Fibre -  
 768 Reinforced geopolymer composite. *Applied Clay Science* 143:125-133. DOI:  
 769 <https://doi.org/10.1016/j.clay.2017.03.030>.
- 770 Alshaaer M., Zaharaki D., Komnitsas K. (2015) Microstructural characteristics and adsorption potential  
 771 of a zeolitic tuff–metakaolin geopolymer. *Desalination and Water Treatment* 56:338-345.
- 772 Ancora R., Borsa M., Cassar L. (2012) Titanium dioxide based photocatalytic composites and derived  
 773 products on a metakaolin support, Google Patents.
- 774 Andrejkovičová S., Sudagar A., Rocha J., Patinha C., Hajjaji W., da Silva E.F., Velosa A., Rocha F.  
 775 (2016) The effect of natural zeolite on microstructure, mechanical and heavy metals adsorption  
 776 properties of metakaolin based geopolymers. *Applied Clay Science* 126:141-152.
- 777 Azimi A., Azari A., Rezakazemi M., Ansarpour M. (2017) Removal of Heavy Metals from Industrial  
 778 Wastewaters: A Review. *ChemBioEng Reviews* 4:37-59. DOI: [doi:10.1002/cben.201600010](https://doi.org/10.1002/cben.201600010).
- 779 Bakharev T. (2005) Resistance of geopolymer materials to acid attack. *Cement and Concrete Research*  
 780 35:658-670. DOI: <https://doi.org/10.1016/j.cemconres.2004.06.005>.

- 781 Bakri A.M.M.A., Kamarudin H., Bnhussain M., Nizar I.K. (2011) Mechanism and Chemical Reaction of  
 782 Fly Ash Geopolymer Cement- A Review. *Journal of Asian Scientific Research* 1:247-253.
- 783 Batool F., Akbar J., Iqbal S., Noreen S., Bukhari S.N.A. (2018) Study of Isothermal, Kinetic, and  
 784 Thermodynamic Parameters for Adsorption of Cadmium: An Overview of Linear and Nonlinear  
 785 Approach and Error Analysis. *Bioinorganic Chemistry and Applications* 2018:11. DOI:  
 786 10.1155/2018/3463724.
- 787 Bernal S.A., Rodríguez E.D., Mejía de Gutiérrez R., Gordillo M., Provis J.L. (2011) Mechanical and  
 788 thermal characterisation of geopolymers based on silicate-activated metakaolin/slag blends.  
 789 *Journal of Materials Science* 46:5477. DOI: 10.1007/s10853-011-5490-z.
- 790 Bignozzi M.C., Manzi S., Lancellotti I., Kamseu E., Barbieri L., Leonelli C. (2013) Mix-design and  
 791 characterization of alkali activated materials based on metakaolin and ladle slag. *Applied Clay*  
 792 *Science* 73:78-85.
- 793 Bortnovsky O., Bezucha P., Sazama P., Dědeček J.Ā., Tvarůžková Z., Sobalik Z.k. (2010) Novel  
 794 Applications of Metal-Geopolymers. *Ceramic Engineering & Science Proceedings* 31:69-82.
- 795 Burakov A.E., Galunin E.V., Burakova I.V., Kucherova A.E., Agarwal S., Tkachev A.G., Gupta V.K.  
 796 (2017) Adsorption of heavy metals on conventional and nanostructured materials for wastewater  
 797 treatment purposes: A review. *Ecotoxicology & Environmental Safety* 148:702.
- 798 Carsten K. (2013) Metakaolin based geopolymers to encapsulate nuclear waste. Imperial College London.
- 799 CĂTĂNESCU I., Georgescu M., Melinescu A. (2012) SYNTHESIS AND CHARACTERIZATION OF  
 800 GEOPOLYMER BINDERS FROM FLY ASH. *Upb Scientific Bulletin* 74.
- 801 Černý Z., Jakubec I., Bezdička P., Štengl V. (2009) PREPARATION OF PHOTOCATALYTIC  
 802 LAYERS BASED ON GEOPOLYMER. *Ceramic Engineering & Science Proceedings* 29.
- 803 Chen L., Zheng K., Liu Y. (2017) Geopolymer-supported photocatalytic TiO<sub>2</sub> film: Preparation and  
 804 characterization. *Construction and Building Materials* 151:63-70.
- 805 Chen Y.L., Tong Y.Y., Pan R.W., Tang J. (2013) The Research on Adsorption Behaviors and  
 806 Mechanisms of Geopolymers on Sr<sup>2+</sup>, Co<sup>2+</sup> and Cs<sup>+</sup>, *Advanced Materials Research, Trans Tech*  
 807 *Publ.* pp. 313-318.
- 808 Cheng T., Chiu J. (2003) Fire-resistant geopolymer produced by granulated blast furnace slag. *Minerals*  
 809 *Engineering* 16:205-210.
- 810 Cheng T., Lee M., Ko M., Ueng T., Yang S. (2012) The heavy metal adsorption characteristics on  
 811 metakaolin-based geopolymer. *Applied Clay Science* 56:90-96.
- 812 Cioffi R., Maffucci L., Santoro L. (2003) Optimization of geopolymer synthesis by calcination and  
 813 polycondensation of a kaolinitic residue. *Resources, Conservation and Recycling* 40:27-38.
- 814 Davidovits J. (1976) Solid phase synthesis of a mineral blockpolymer by low temperature  
 815 polycondensation of aluminosilicate polymers, IUPAC International Symposium on  
 816 Macromolecules, Stockholm.
- 817 Davidovits J. (1994) Properties of geopolymer cements, First international conference on alkaline  
 818 cements and concretes, Scientific Research Institute on Binders and Materials Kiev State  
 819 Technical University, Ukraine. pp. 131-149.
- 820 Deb P.S., Nath P., Sarker P.K. (2014) The effects of ground granulated blast-furnace slag blending with  
 821 fly ash and activator content on the workability and strength properties of geopolymer concrete  
 822 cured at ambient temperature. *Materials & Design* (1980-2015) 62:32-39. DOI:  
 823 <https://doi.org/10.1016/j.matdes.2014.05.001>.
- 824 Diercks M., Sand W., Bock E. (1991) Microbial corrosion of concrete. *Experientia. Experientia* 47:514-  
 825 516.
- 826 Djobo J.N.Y., Tchadjé L.N., Tchakoute H.K., Kenne B.B.D., Elimbi A., Njopwouo D. (2014) Synthesis  
 827 of geopolymer composites from a mixture of volcanic scoria and metakaolin. *Journal of Asian*  
 828 *Ceramic Societies* 2:387-398. DOI: <https://doi.org/10.1016/j.jascr.2014.08.003>.
- 829 Duan P., Yan C., Zhou W., Ren D. (2016) Development of fly ash and iron ore tailing based porous  
 830 geopolymer for removal of Cu (II) from wastewater. *Ceramics International* 42:13507-13518.

- 831 Duxson P., Fernández-Jiménez A., Provis J.L., Lukey G.C., Palomo A., van Deventer J.S.J. (2007a)  
 832 Geopolymer technology: the current state of the art. *Journal of Materials Science* 42:2917-2933.  
 833 DOI: 10.1007/s10853-006-0637-z.
- 834 Duxson P., Lukey G.C., Separovic F., van Deventer J.S.J. (2005) Effect of Alkali Cations on Aluminum  
 835 Incorporation in Geopolymeric Gels. *Industrial & Engineering Chemistry Research* 44:832-839.  
 836 DOI: 10.1021/ie0494216.
- 837 El-Geundi M.S. (1991) Homogeneous surface diffusion model for the adsorption of basic dyestuffs onto  
 838 natural clay in batch adsorbers. *Adsorption Science & Technology* 8:217-225.
- 839 Emery J. (1992) Mineral aggregate conservation-reuse and recycling. Queen's Printer for Ontario:  
 840 Ontario Ministry of Natural Resources (MNR).
- 841 Fabbri B., Gualtieri S., Leonardi C. (2013) Modifications induced by the thermal treatment of kaolin and  
 842 determination of reactivity of metakaolin. *Applied Clay Science* 73:2-10.
- 843 Falah M. (2015) Synthesis of New Composites of Inorganic Polymers (Geopolymers) with Metal Oxide  
 844 Nanoparticles and their Photodegradation of Organic Pollutants.  
 845 *URI: http://hdl.handle.net/10063/4847*
- 846 Falah M., MacKenzie K.J., Knibbe R., Page S.J., Hanna J.V. (2016) New composites of nanoparticle Cu  
 847 (I) oxide and titania in a novel inorganic polymer (geopolymer) matrix for destruction of dyes and  
 848 hazardous organic pollutants. *Journal of hazardous materials* 318:772-782.
- 849 Fallah M., MacKenzie K.J.D., Hanna J.V., Page S.J. (2015) Novel photoactive inorganic polymer  
 850 composites of inorganic polymers with copper(I) oxide nanoparticles. *Journal of Materials*  
 851 *Science* 50:7374-7383. DOI: 10.1007/s10853-015-9295-3.
- 852 Faqir N.M., Shawabkeh R., Al-Harathi M., Wahhab H.A. (2018) Fabrication of Geopolymers from  
 853 Untreated Kaolin Clay for Construction Purposes. *Geotechnical and Geological Engineering*.  
 854 DOI: 10.1007/s10706-018-0597-5.
- 855 Fhwa U.S. (1998) User Guidelines for Waste and Byproduct Materials in Pavement Construction. Costs.
- 856 Gasparini E., Tarantino S.C., Ghigna P., Riccardi M.P., Cedillo-González E.I., Siligardi C., Zema M.  
 857 (2013) Thermal dehydroxylation of kaolinite under isothermal conditions. *Applied Clay Science*  
 858 80-81:417-425. DOI: <https://doi.org/10.1016/j.clay.2013.07.017>.
- 859 Ge Y., Cui X., Kong Y., Li Z., He Y., Zhou Q. (2015a) Porous geopolymeric spheres for removal of Cu  
 860 (II) from aqueous solution: synthesis and evaluation. *Journal of hazardous materials* 283:244-  
 861 251.
- 862 Ge Y., Cui X., Liao C., Li Z. (2017) Facile fabrication of green geopolymer/alginate hybrid spheres for  
 863 efficient removal of Cu (II) in water: Batch and column studies. *Chemical Engineering Journal*  
 864 311:126-134.
- 865 Ge Y., Yuan Y., Wang K., He Y., Cui X. (2015b) Preparation of geopolymer-based inorganic membrane  
 866 for removing Ni<sup>2+</sup> from wastewater. *Journal of hazardous materials* 299:711-718.
- 867 Geddes D.A., Ke X., Bernal S.A., Hayes M., Provis J.L. (2018) Metakaolin-Based Geopolymers for  
 868 Nuclear Waste Encapsulation, Springer Netherlands, Dordrecht. pp. 183-188.
- 869 Hamaideh A., Komnitsas K., Esaifan M., Al-Kafawein J.A.K., Rahier H., Alshaaer M. (2014) Advantages  
 870 of Applying a Steam Curing Cycle for the Production of Kaolinite-Based Geopolymers. *Arabian*  
 871 *Journal for Science & Engineering* 39:7591-7597.
- 872 Hashimoto S., Machino T., Takeda H., Daiko Y., Honda S., Iwamoto Y. (2015) Antimicrobial activity of  
 873 geopolymers ion-exchanged with copper ions. *Ceramics International* 41:13788-13792.
- 874 Heah C.Y., Kamarudin H., Al Bakri A.M., Bnhussain M., Luqman M., Nizar I.K., Ruzaidi C.M., Liew Y.  
 875 (2013) Kaolin-based geopolymers with various NaOH concentrations. *International Journal of*  
 876 *Minerals, Metallurgy, and Materials* 20:313-322.
- 877 Hoy M., Horpibulsuk S., Arulrajah A. (2016) Strength development of Recycled Asphalt Pavement-Fly  
 878 ash geopolymer as a road construction material. *Construction & Building Materials* 117:209-219
- 879 Hu S., Wang H., Zhang G., Ding Q. (2008) Bonding and abrasion resistance of geopolymeric repair  
 880 material made with steel slag. *Cement & Concrete Composites* 30:239-244.

- 881 Husem M. (2006) The effects of high temperature on compressive and flexural strengths of ordinary and  
882 high-performance concrete. *Fire Safety Journal* 41:155-163.
- 883 Islander R.L., Deviny J.S., Mansfeld F., Postyn A., Hong S. (1991) Microbial Ecology of Crown  
884 Corrosion in Sewers. *Journal of Environmental Engineering* 117:751-770.
- 885 Itodo A., Abdulrahman F., Hassan L., Maigandi S., Itodo H. (2010) Intraparticle diffusion and  
886 intraparticulate diffusivities of herbicide on derived activated carbon. *Researcher* 2:74-86.
- 887 Izquierdo M., Querol X., Davidovits J., Antenucci D., Nugteren H., Fernández-Pereira C. (2009) Coal fly  
888 ash-slag-based geopolymers: microstructure and metal leaching. *Journal of hazardous materials*  
889 166:561-566.
- 890 Jaarsveld J.G.S.V., Deventer J.S.J.V., Lukey G.C. (2002) The effect of composition and temperature on  
891 the properties of fly ash- and kaolinite-based geopolymers. *Chemical Engineering Journal* 89:63-  
892 73.
- 893 Jaishankar M., Tseten T., Anbalagan N., Mathew B.B., Beeregowda K.N. (2014) Toxicity, mechanism  
894 and health effects of some heavy metals. *Interdiscip Toxicol* 7:60-72.
- 895 Javadian H., Ghorbani F., Tayebi H.-a., Asl S.H. (2015) Study of the adsorption of Cd (II) from aqueous  
896 solution using zeolite-based geopolymer, synthesized from coal fly ash; kinetic, isotherm and  
897 thermodynamic studies. *Arabian Journal of Chemistry* 8:837-849.
- 898 Carsten K. (2013) Metakaolin based geopolymers to encapsulate nuclear waste. Imperial College London.
- 899 Kara İ., Yilmazer D., Akar S.T. (2017) Metakaolin based geopolymer as an effective adsorbent for  
900 adsorption of zinc (II) and nickel (II) ions from aqueous solutions. *Applied Clay Science* 139:54-  
901 63.
- 902 Ke X., Provis J.L., Bernal S.A. (2018) Structural Ordering of Aged and Hydrothermally Cured  
903 Metakaolin Based Potassium Geopolymers.
- 904 Khale D., Chaudhary R. (2007) Mechanism of geopolymerization and factors influencing its  
905 development: a review. *Journal of Materials Science* 42:729-746.
- 906 KIM E.H. (2012) Understanding effects of silicon/aluminum ratio and calcium hydroxide on chemical  
907 composition, nanostructure and compressive strength for metakaolin geopolymers, University of  
908 Illinois at Urbana-Champaign.
- 909 Kljajević L. M., Nenadović S. S., Nenadović M. T., Bundaleski N. K., Todorović B. Ž., Pavlović V. B.,  
910 Rakočević Z. L. (2017) Structural and chemical properties of thermally treated geopolymer  
911 samples. *Ceramics International* 43:6700-6708.
- 912 Kovářik T., Křenek T., Pola M., Rieger D., Kadlec J., Franče P. (2017) Ceramic-like open-celled  
913 geopolymer foam as a porous substrate for water treatment catalyst 175:012044.
- 914 López F.J., Sugita S., Kobayashi T. (2013) Cesium-adsorbent geopolymer foams based on silica from rice  
915 husk and metakaolin. *Chemistry Letters* 43:128-130.
- 916 López F.J., Sugita S., Tagaya M., Kobayashi T. (2014) Metakaolin-Based Geopolymers for Targeted  
917 Adsorbents to Heavy Metal Ion Separation. *Journal of Materials Science and Chemical*  
918 *Engineering* Vol.02No.07:12. DOI: 10.4236/msce.2014.27002.
- 919 Lata S., Singh P.K., Samadder S.R. (2015) Regeneration of adsorbents and recovery of heavy metals: a  
920 review. *International Journal of Environmental Science and Technology* 12:1461-1478. DOI:  
921 10.1007/s13762-014-0714-9.
- 922 Lee N.K., Khalid H.R., Lee H.K. (2016) Synthesis of mesoporous geopolymers containing zeolite phases  
923 by a hydrothermal treatment. *Microporous and Mesoporous Materials* 229:22-30. DOI:  
924 <https://doi.org/10.1016/j.micromeso.2016.04.016>.
- 925 Lee N.K., Khalid H.R., Lee H.K. (2017) Adsorption characteristics of cesium onto mesoporous  
926 geopolymers containing nano-crystalline zeolites. *Microporous and Mesoporous Materials*  
927 242:238-244. DOI: <https://doi.org/10.1016/j.micromeso.2017.01.030>.

- 928 Li C.M., He Y., Tang Q., Wang K.T., Cui X.M. (2016) Study of the preparation of CdS on the surface of  
 929 geopolymer spheres and photocatalyst performance. *Materials Chemistry & Physics* 178:204-  
 930 210.
- 931 Liu Y., Yan C., Zhang Z., Wang H., Zhou S., Zhou W. (2016) A comparative study on fly ash,  
 932 geopolymer and faujasite block for Pb removal from aqueous solution. *Fuel* 185:181-189.
- 933 Luukkonen T., Runtti H., Niskanen M., Tolonen E.-T., Sarkkinen M., Kemppainen K., Rämö J., Lassi U.  
 934 (2016) Simultaneous removal of Ni (II), As (III), and Sb (III) from spiked mine effluent with  
 935 metakaolin and blast-furnace-slag geopolymers. *Journal of environmental management* 166:579-  
 936 588.
- 937 Luukkonen T., Tolonen E.-T., Runtti H., Kemppainen K., Perämäki P., Rämö J., Lassi U. (2017)  
 938 Optimization of the metakaolin geopolymer preparation for maximized ammonium adsorption  
 939 capacity. *Journal of Materials Science* 52:9363-9376. DOI: 10.1007/s10853-017-1156-9.
- 940 Ma Y., Hu J., Ye G. (2013) The pore structure and permeability of alkali activated fly ash. *Fuel* 104:771-  
 941 780.
- 942 Masliana M., Kenneth J., Meor Yusoff M. (2013) DEGRADATION OF METHYLENE BLUE VIA  
 943 GEOPOLYMER COMPOSITE PHOTOCATALYSIS. *Solid State Science and Technology*, Vol.  
 944 21, No 1 & 2 23-30.
- 945 McGannon H.E. (1971) The making, shaping and treating of steel. United States Steel
- 946 Motorwala A., Shah V., Kammula R., Nannapaneni P., Rajiwala P. (2008) ALKALI activated FLY-ASH  
 947 based geopolymer concrete. *International journal of emerging technology and advanced*  
 948 *engineering*:159-166.
- 949 Moya J.S., Cabal B.n., Sanz J.s., Torrecillas R.n. (2013) Metakaolin-Nanosilver as Biocide Agent in  
 950 Geopolymer. *Ceramic Engineering & Science Proceedings* 33:3-11.
- 951 Murray H.H. (2006a) Chapter 2 Structure and Composition of the Clay Minerals and their Physical and  
 952 Chemical Properties. *Developments in Clay Science. Elsevier Ltd*,7-31.
- 953 Mužek M.N., Svilović S., Zelić J. (2014) Fly ash-based geopolymeric adsorbent for copper ion removal  
 954 from wastewater. *Desalination and Water Treatment* 52:2519-2526.
- 955 Naghsh M., Shams K. (2017) Synthesis of a kaolin-based geopolymer using a novel fusion method and its  
 956 application in effective water softening. *Applied Clay Science* 146:238-245.
- 957 Noor ul A., Faisal M., Muhammad K., gul S. (2016) Synthesis and characterization of geopolymer from  
 958 bagasse bottom ash, waste of sugar industries and naturally available china clay. *Journal of*  
 959 *Cleaner Production* 129:491-495. DOI: <https://doi.org/10.1016/j.jclepro.2016.04.024>.
- 960 Novais R.M., Ascensão G., Tobaldi D.M., Seabra M.P., Labrincha J.o.A. (2018) Biomass fly ash  
 961 geopolymer monoliths for effective methylene blue removal from wastewaters. *Journal of*  
 962 *Cleaner Production* 171:783-794.
- 963 Novais R.M., Buruberri L., Seabra M., Labrincha J. (2016) Novel porous fly-ash containing geopolymer  
 964 monoliths for lead adsorption from wastewaters. *Journal of hazardous materials* 318:631-640.
- 965 Nur Q.A., Sari N.U., Harianti, Subaer, Nur Q.A., Sari N.U., Harianti, Subaer, Nur Q.A., Sari N.U. (2017)  
 966 Development of Geopolymers Composite Based on Metakaolin-Nano ZnO for Antibacterial  
 967 Application. *Mater. Sci. Eng.* 180:012289. <http://iopscience.iop.org/1757-899X/180/1/012289>
- 968 Ofer-Rozovsky E., Arbel Haddad M., Bar Nes G., Katz A. (2016) The formation of crystalline phases in  
 969 metakaolin-based geopolymers in the presence of sodium nitrate. *Journal of Materials Science*  
 970 51:4795-4814. DOI: 10.1007/s10853-016-9767-0.
- 971 Ogundiran M.B., Enakerakpo I.S. (2018) Metakaolin clay-derived geopolymer for recycling of waste  
 972 cathode ray tube glass. *Academic Journals* 12(6):42-49. <https://doi.org/10.5897/AJPAC2018.0759>
- 973 Okoye F.N., Durgaprasad J., Singh N.B. (2016) Effect of silica fume on the mechanical properties of fly  
 974 ash based-geopolymer concrete. *Ceramics International* 42:3000-3006. DOI:  
 975 <https://doi.org/10.1016/j.ceramint.2015.10.084>.
- 976 Pacheco-Torgal F., Castro-Gomes J., Jalali S. (2008) Alkali-activated binders: A review: Part 1.  
 977 Historical background, terminology, reaction mechanisms and hydration products. *Construction*  
 978 *and Building Materials* 22:1305-1314.

- 979 Panda B., Paul S.C., Hui L.J., Tay Y.W.D., Tan M.J. (2017) Additive manufacturing of geopolymer for  
 980 sustainable built environment. *Journal of Cleaner Production* 167:281-288. DOI:  
 981 <https://doi.org/10.1016/j.jclepro.2017.08.165>.
- 982 Pelisser F., Guerrino E.L., Menger M., Michel M.D., Labrincha J.A. (2013) Micromechanical  
 983 characterization of metakaolin-based geopolymers. *Construction and Building Materials* 49:547-  
 984 553. DOI: 10.1016/j.conbuildmat.2013.08.081.
- 985 Perera D., Blackford M., R Vance E., V Hanna J., Finnie K., L Nicholson C. (2011) Geopolymers for the  
 986 Immobilization of Radioactive Waste. *Mat. Res. Soc. Symp. Proc.* 824
- 987 Prachasaree W., Limkatanyu S., Hawa A., Samakrattakit A. (2014) Development of Equivalent Stress  
 988 Block Parameters for Fly-Ash-Based Geopolymer Concrete. *Arabian Journal for Science and*  
 989 *Engineering* 39:8549-8558. DOI: 10.1007/s13369-014-1447-2.
- 990 Pratama M.A. (2017) The Properties of Nano Silver (Ag)-Geopolymer as Antibacterial Composite for  
 991 Functional Surface Materials, Ags1 & Migs 3\_engineering Technology International Conference.  
 992 *MATEC Web of Conferences* 97, 01010. DOI: 10.1051/mateconf/20179701010.
- 993 Proctor D., Fehling K., Shay E., Wittenborn J., Green J., Avent C., Bigham R., Connolly M., Lee B.,  
 994 Shepker T. (2000) Physical and chemical characteristics of blast furnace, basic oxygen furnace,  
 995 and electric arc furnace steel industry slags. *Environmental Science & Technology* 34:1576-1582.
- 996 Rahman M., Law D., Patnaikuni I. (2016) Optimizing the mix design of clay based geopolymer concrete,  
 997 ASEA-SEC-3 2016: *Integrated Solutions for Infrastructure Development*, ISEC Press. pp. 1-6.
- 998 Rasaki S.A., Zhang B., Liu S., Thomas T., Yang M. (2018) Nanourchin ZnO@TiCN composites for Cr  
 999 (VI) adsorption and thermochemical remediation. *Journal of Environmental Chemical*  
 1000 *Engineering* 6( 4): 3837-3848. <https://doi.org/10.1016/j.jece.2018.05.040>
- 1001 Richardson G.N., Zhao A. (2010) Geosynthetic Fundamentals in Landfill Design. *Advances in*  
 1002 *Environmental Geotechnics*.pp.275-285
- 1003 Robayo R.A., Gutiérrez R.M.a.D., Gordillo M. (2016) Natural pozzolan-and granulated blast furnace  
 1004 slag-based binary geopolymers. *Materiales De Construcción* 66:e077.
- 1005 Rovnanik P. (2010) Effect of curing temperature on the development of hard structure of metakaolin-  
 1006 based geopolymer. *Construction & Building Materials* 24:1176-1183.
- 1007 Rowe R.K. (2007) Advances and Remaining Challenges for Geosynthetics in Geoenvironmental  
 1008 Engineering Applications. *Soils & Rocks* 30(1)
- 1009 Rubio-Avalos J.C. (2018) Antibacterial Metakaolin-Based Geopolymer Cement. *Calcined Clays for*  
 1010 *Sustainable Concrete* pp 398-403
- 1011 Rui M.N., Ascensão G., Tobaldi D.M., Seabra M.P., Labrincha J.o.A. (2018) Biomass fly ash geopolymer  
 1012 monoliths for effective methylene blue removal from wastewaters. *Journal of Cleaner Production*  
 1013 171.
- 1014 Salwa S. S. M., M Mustafa A., Abdullah M.M.A.B., Kamarudin H., Ruzaidi C., Binhussain M., Syed  
 1015 Zuber S.Z. (2013) Review on Current Geopolymer as a Coating Material. *Australian Journal of Basic and*  
 1016 *Applied Sciences* 7(5):246-257
- 1017 Saheb V. (2012) Studies on Blast Furnace Slag Flow Characteristics. (*Thesis*) National Institute of  
 1018 Technology, Rourkela
- 1019 Samal S., Thanh N.P., Marvalova B., Petrikova I. (2017) Thermal Characterization of Metakaolin-Based  
 1020 Geopolymer. *JOM* 69:2480-2484. DOI: 10.1007/s11837-017-2555-8.
- 1021 Samantasinghar S., Singh S.P. (2018) Effect of synthesis parameters on compressive strength of fly ash-  
 1022 slag blended geopolymer. *Construction and Building Materials* 170:225-234. DOI:  
 1023 <https://doi.org/10.1016/j.conbuildmat.2018.03.026>.
- 1024 Sarkar C., Basu J.K., Samanta A.N. (2017) Removal of Ni<sup>2+</sup> ion from waste water by Geopolymeric  
 1025 Adsorbent derived from LD Slag. *Journal of Water Process Engineering* 17:237-244.
- 1026 Sarkar M., Maiti M., Maiti S., Xu S., Li Q. (2018) ZnO-SiO<sub>2</sub> nanohybrid decorated sustainable  
 1027 geopolymer retaining anti-biodeterioration activity with improved durability. *Materials Science*  
 1028 *and Engineering: C* 92:663-672. DOI: <https://doi.org/10.1016/j.msec.2018.07.005>.

- 1029 Sazama P., Bortnovsky O., Dědeček J.Ā., Tvarůžková Z., Sobalík Z.k. (2011) Geopolymer based  
1030 catalysts—New group of catalytic materials. *Catalysis Today* 164:92-99.
- 1031 Seynou M., Millogo Y., Zerbo L., Sanou I., Ganon F.o., Ouedraogo R., Kaboré K. (2016) Production and  
1032 Characterization of Pozzolan with Raw Clay from Burkina Faso. *Journal of Minerals &*  
1033 *Materials Characterization & Engineering* 04:195-209.
- 1034 Singh B., Ishwarya G., Gupta M., Bhattacharyya S.K. (2015) Geopolymer concrete: A review of some  
1035 recent developments. *Construction & Building Materials* 85:78-90.
- 1036 Singhal A., Gangwar B.P., Gayathry J.M. (2017) CTAB modified large surface area nanoporous  
1037 geopolymer with high adsorption capacity for copper ion removal. *Applied Clay Science* 150:106-  
1038 114.
- 1039 Siyal A.A., Shamsuddin M.R., Khan M.I., Rabat N.E., Zulfiqar M., Man Z., Siame J., Azizli K.A. (2018)  
1040 A review on geopolymers as emerging materials for the adsorption of heavy metals and dyes.  
1041 *Journal of Environmental Management* 224:327-339. DOI:  
1042 <https://doi.org/10.1016/j.jenvman.2018.07.046>.
- 1043 Srinivasan K., Sivakumar A. (2013) Geopolymer Binders: A Need for Future Concrete Construction. *Isrn*  
1044 *Polymer Science*. <http://dx.doi.org/10.1155/2013/509185>
- 1045 Stojanovic B.D., Dzunuzovic A.S., Ilic N.I. (2018) 17 - Review of methods for the preparation of  
1046 magnetic metal oxides, in: B. D. Stojanovic (Ed.), *Magnetic, Ferroelectric, and Multiferroic*  
1047 *Metal Oxides*, Elsevier. pp. 333-359.
- 1048 Strini A., Roviello G., Ricciotti L., Ferone C., Messina F., Schiavi L., Corsaro D., Cioffi R. (2016a) TiO<sub>2</sub>-  
1049 Based Photocatalytic Geopolymers for Nitric Oxide Degradation. *Materials* 9:513.
- 1050 Sturm P., Gluth G.J.G., Brouwers H.J.H., Kühne H.C. (2016) Synthesizing one-part geopolymers from  
1051 rice husk ash. *Construction and Building Materials* 124:961-966. DOI:  
1052 <https://doi.org/10.1016/j.conbuildmat.2016.08.017>.
- 1053 Tang Q., Ge Y.-y., Wang K.-t., He Y., Cui X.-m. (2015) Preparation and characterization of porous  
1054 metakaolin-based inorganic polymer spheres as an adsorbent. *Materials & Design* 88:1244-1249.  
1055 DOI: <https://doi.org/10.1016/j.matdes.2015.09.126>.
- 1056 Tang Q., He Y., Wang Y.-p., Wang K.-t., Cui X.-m. (2016) Study on synthesis and characterization of  
1057 ZSM-20 zeolites from metakaolin-based geopolymers. *Applied Clay Science* 129:102-107. DOI:  
1058 <https://doi.org/10.1016/j.clay.2016.05.011>.
- 1059 Temujin J., Minjigmaa A., Rickard W., Lee M., Williams I., van Riessen A. (2009) Preparation of  
1060 metakaolin based geopolymer coatings on metal substrates as thermal barriers. *Applied Clay*  
1061 *Science* 46:265-270. DOI: <https://doi.org/10.1016/j.clay.2009.08.015>.
- 1062 Timakul P., Rattanaprasit W., Aungkavattana P. (2016) Enhancement of compressive strength and  
1063 thermal shock resistance of fly ash-based geopolymer composites. *Construction and Building*  
1064 *Materials* 121:653-658. DOI: <https://doi.org/10.1016/j.conbuildmat.2016.06.037>.
- 1065 Tognonvi M.T., Soro J., Rossignol S. (2012) Physical-chemistry of silica/alkaline silicate interactions  
1066 during consolidation. Part 1: Effect of cation size. *Journal of Non-Crystalline Solids* 358:81-87.
- 1067 Trivunac K., Kljajević L., Nenadović S., Gulicovski J., Mirković M., Babić B., Stevanović S. (2016)  
1068 Microstructural characterization and adsorption properties of alkali-activated materials based on  
1069 metakaolin. *Science of Sintering* 48:209-220.
- 1070 Villaquirán-Cacedo M.n.A., Gutiérrez R.M.a. (2015) Synthesis of ternary geopolymers based on  
1071 metakaolin, boiler slag and rice husk ash. *Dyna (Medellin, Colombia)* 82(194):104-110.  
1072 DOI:10.15446/dyna.v82n194.46352
- 1073 Vu T.H., Tran M.V. (2018) A Review on Immobilisation of Toxic Wastes Using Geopolymer Technique,  
1074 *Springer Singapore, Singapore*. pp. 299-309.
- 1075 Wang H., Chen Z., Deng X., Wu S., Yu Q., Yang W., Zhou J. (2018) Template-Free Synthesis of  
1076 Macroporous SiO<sub>2</sub> Catalyst Supports for Diesel Soot Combustion. *Industrial & Engineering*  
1077 *Chemistry Research* 57:11600-11607. DOI: 10.1021/acs.iecr.8b02746.

- 1078 Wei S., Sanchez M., Trejo D., Gillis C. (2010) Microbial mediated deterioration of reinforced concrete  
 1079 structures. *International Biodeterioration & Biodegradation* 64:748-754.
- 1080 Xu H., Deventer J.S.J.V. (2000) The geopolymerisation of aluminosilicate minerals. *International*  
 1081 *Journal of Mineral Processing* 59:247-266.
- 1082 Xu H., Deventer J.S.J.V. (2003) The effect of alkali metals on the formation of geopolymeric gels from  
 1083 alkali-feldspars. *Colloids & Surfaces A Physicochemical & Engineering Aspects* 216:27-44.
- 1084 Xu H., Gong W., Syltebo L., Izzo K., Lutze W., Pegg I.L. (2014) Effect of blast furnace slag grades on fly  
 1085 ash based geopolymer waste forms. *Fuel* 133:332-340.
- 1086 Yao J.Z., Li C.L., Lu L.N., Bing L.W. (2013) A facile and low-cost synthesis of granulated blast furnace  
 1087 slag-based cementitious material coupled with Fe<sub>2</sub>O<sub>3</sub> catalyst for treatment of dye wastewater.  
 1088 *Applied Catalysis B Environmental* 138:9-16.
- 1089 Yao X., Zhang Z., Zhu H., Chen Y. (2009) Geopolymerization process of alkali-metakaolinite  
 1090 characterized by isothermal calorimetry. *Thermochimica Acta* 493:49-54. DOI:  
 1091 <https://doi.org/10.1016/j.tca.2009.04.002>.
- 1092 Yip C.K., Lukey G.C., Dean J.S. (2004) Effect of blast furnace slag addition on microstructure and  
 1093 properties of metakaolinite geopolymeric materials. *Advances in Ceramic Matrix Composites IX*,  
 1094 Volume 153:187-209.
- 1095 Yousef R.I., El-Eswed B., Alshaaer M., Khalili F., Rahier H. (2012) Degree of reactivity of two kaolinitic  
 1096 minerals in alkali solution using zeolitic tuff or silica sand filler. *Ceramics International* 38:5061-  
 1097 5067.
- 1098 Yu J., Li X., Fleming D., Meng Z., Wang D., Tahmasebi A. (2012) Analysis on Characteristics of Fly  
 1099 Ash from Coal Fired Power Stations. *Energy Procedia* 17:3-9. DOI:  
 1100 <https://doi.org/10.1016/j.egypro.2012.02.054>.
- 1101 Zahid M., Shafiq N., Jalal A. (2018) Investigating the effects of solar cure curing method on the  
 1102 compressive strength, microstructure and polymeric reaction of fly ash based geopolymer.  
 1103 *Construction and Building Materials* 181:227-237. DOI:  
 1104 <https://doi.org/10.1016/j.conbuildmat.2018.06.046>.
- 1105 Zhang Y., Liu L. (2013) Fly ash-based geopolymer as a novel photocatalyst for degradation of dye from  
 1106 wastewater. *Particuology* 11:353-358. DOI: <https://doi.org/10.1016/j.partic.2012.10.007>.
- 1107 Zhang Y., Sun W., Li Z. (2008) Synthesis and microstructural characterization of fully-reacted potassium-  
 1108 poly(sialate-Siloxo) geopolymeric cement matrix. *Aci Materials Journal* 105:156-164.
- 1109 Zhang Y.J., He P.Y., Yang M.Y., Kang L. (2017) A new graphene bottom ash geopolymeric composite  
 1110 for photocatalytic H<sub>2</sub> production and degradation of dyeing wastewater. *International Journal of*  
 1111 *Hydrogen Energy* 42: 20589-20598. <https://doi.org/10.1016/j.ijhydene.2017.06.156>
- 1112 Zhang Y.J., He P.Y., Zhang Y.X., Chen H. (2018) A novel electroconductive graphene/fly ash-based  
 1113 geopolymer composite and its photocatalytic performance. *Chemical Engineering Journal*  
 1114 334:2459-2466. DOI: <https://doi.org/10.1016/j.cej.2017.11.171>.
- 1115 Zhang Y.J., Kang L., Liu L.C. (2015) Alkali-activated cements for photocatalytic degradation of organic  
 1116 dyes. pp.729-775. <https://doi.org/10.1533/9781782422884.5.729>
- 1117 Zhang Y.J., Liu L.C., Xu Y., Wang Y.C., Xu D.L. (2012a) A new alkali-activated steel slag-based  
 1118 cementitious material for photocatalytic degradation of organic pollutant from waste water.  
 1119 *Journal of Hazardous Materials* 209-210:146-150. DOI:  
 1120 <https://doi.org/10.1016/j.jhazmat.2012.01.001>.
- 1121 Zhuang X.Y., Chen L., Komarneni S., Zhou C.H., Tong D.S., Yang H.M., Yu W.H., Wang H. (2016) Fly  
 1122 ash-based geopolymer: clean production, properties and applications. *Journal of Cleaner*  
 1123 *Production* 125:253-267. <https://doi.org/10.1016/j.jclepro.2016.03.019>
- 1124 Živica V.r., Balkovic S., Drabik M. (2011) Properties of metakaolin geopolymer hardened paste prepared  
 1125 by high-pressure compaction. *Construction & Building Materials* 25:2206-2213.  
 1126 <https://doi.org/10.1016/j.conbuildmat.2010.11.004>  
 1127

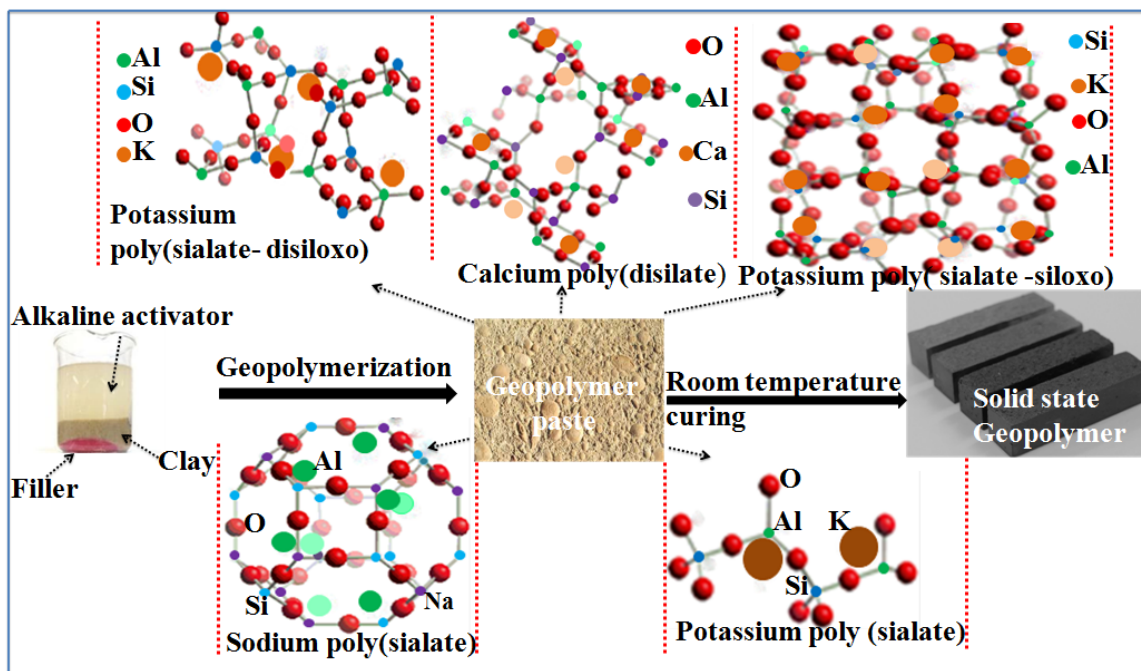


Fig. 1

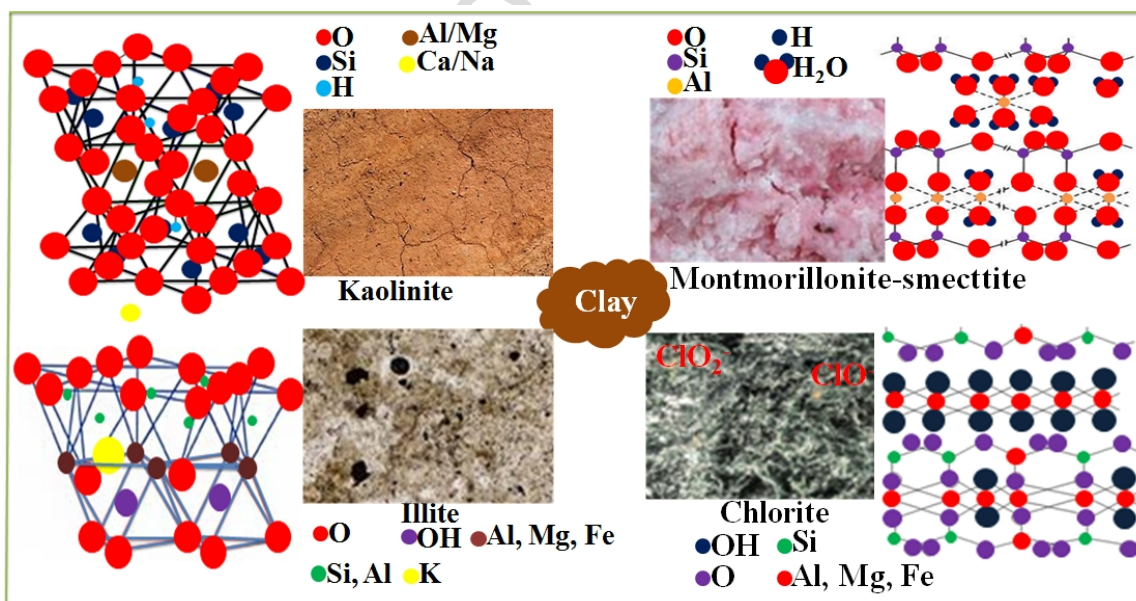


Fig. 2

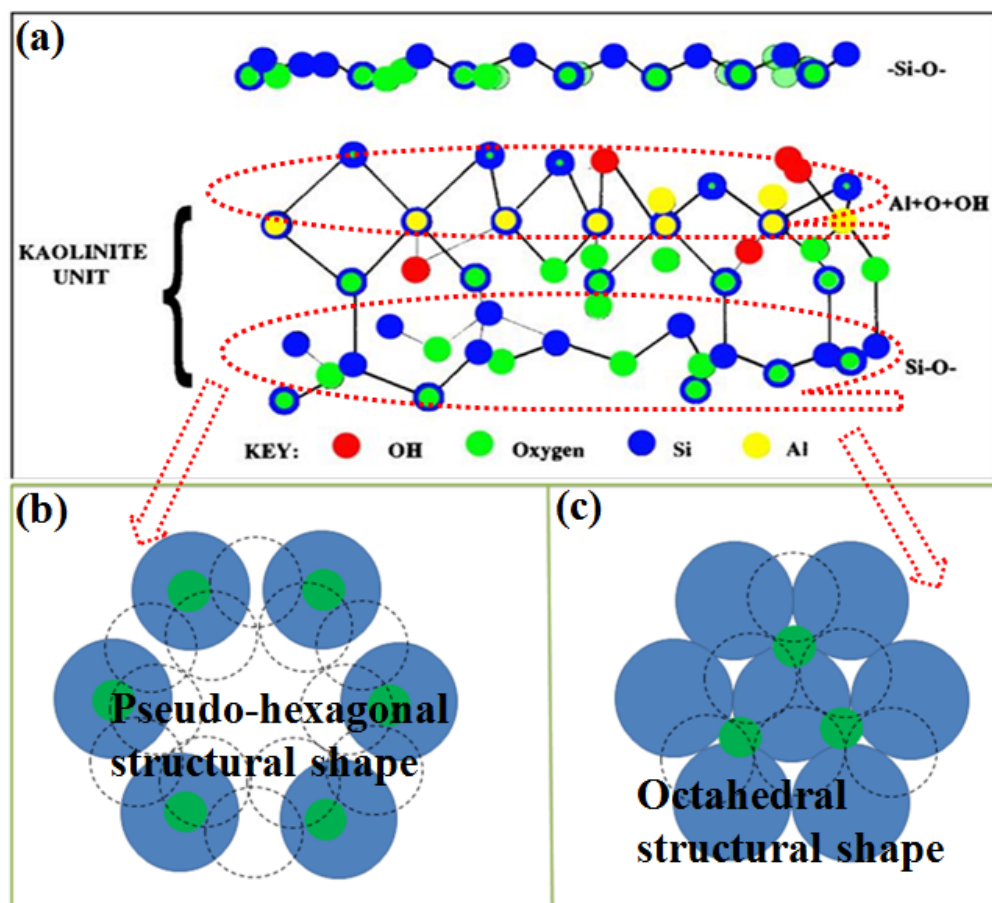


Fig. 3

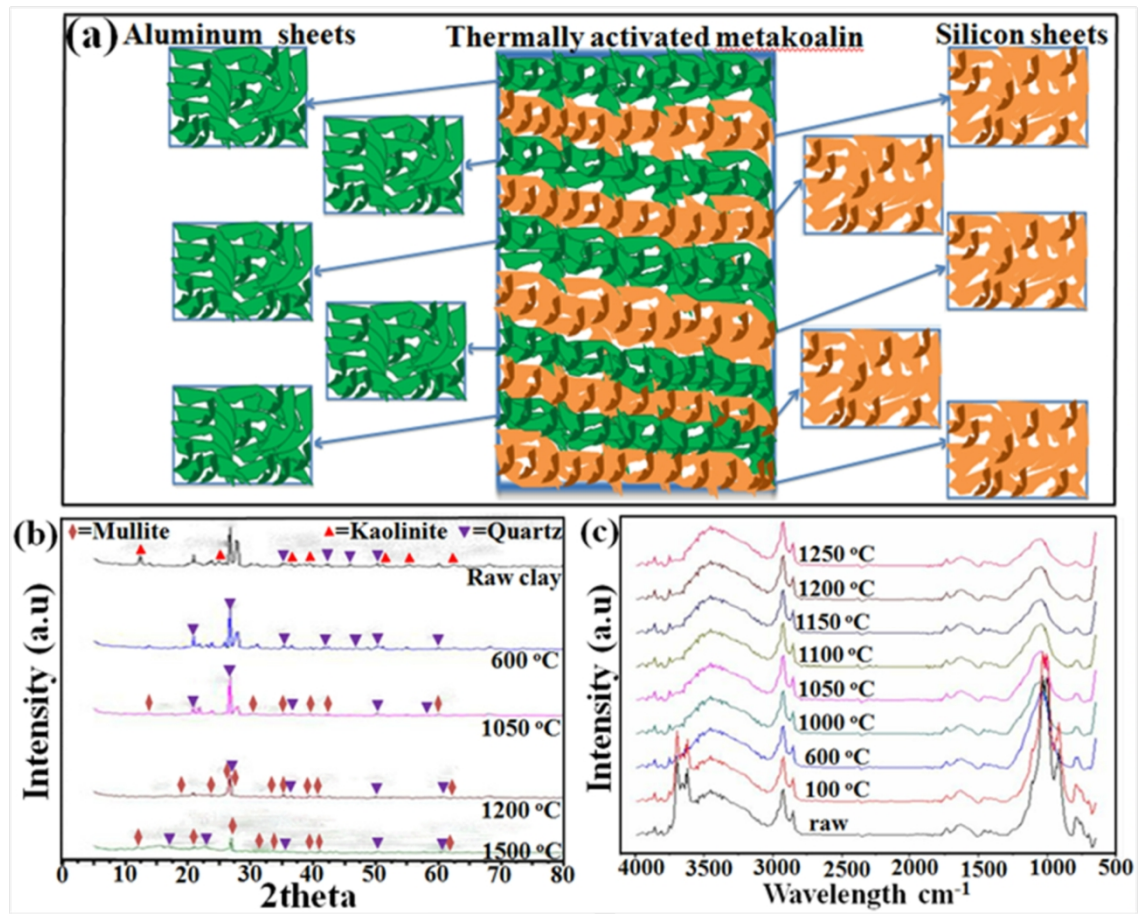


Fig. 4

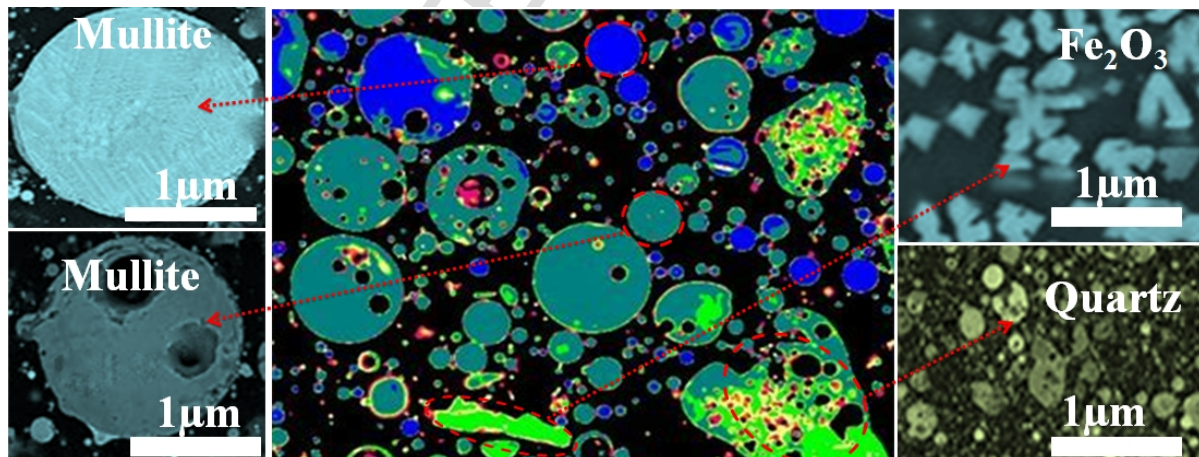


Fig. 5

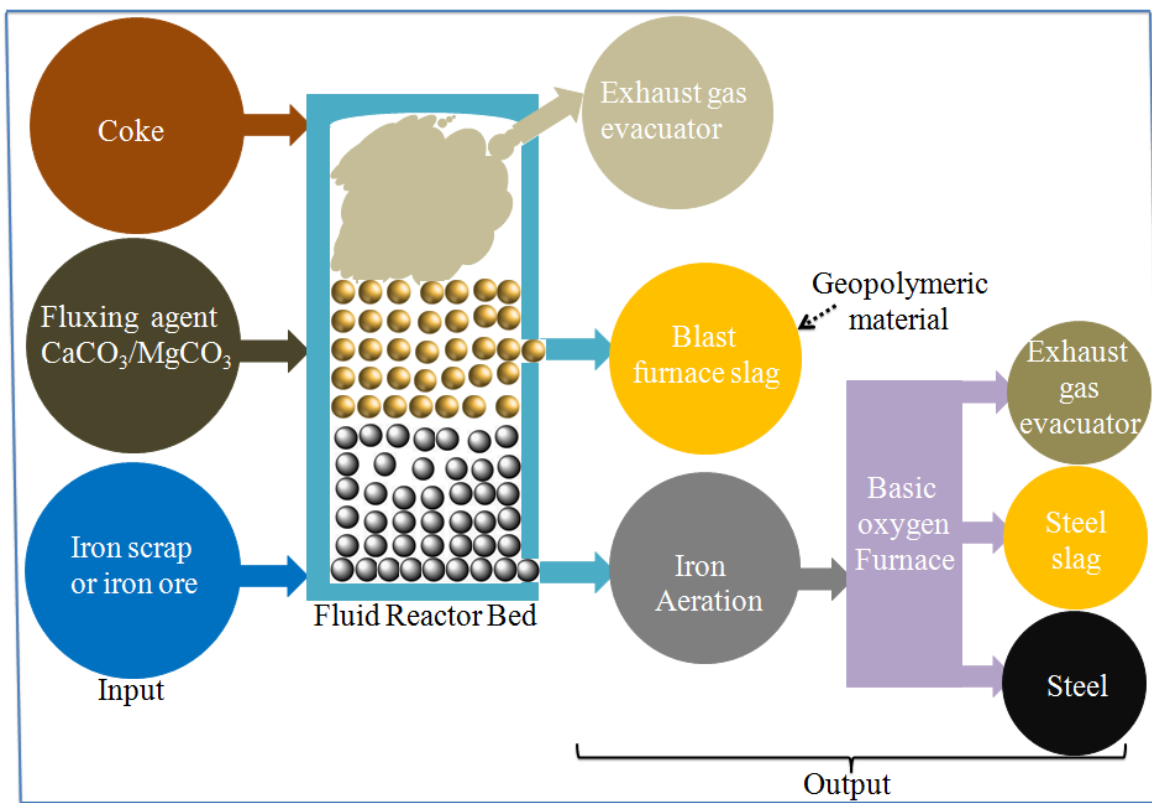


Fig. 6

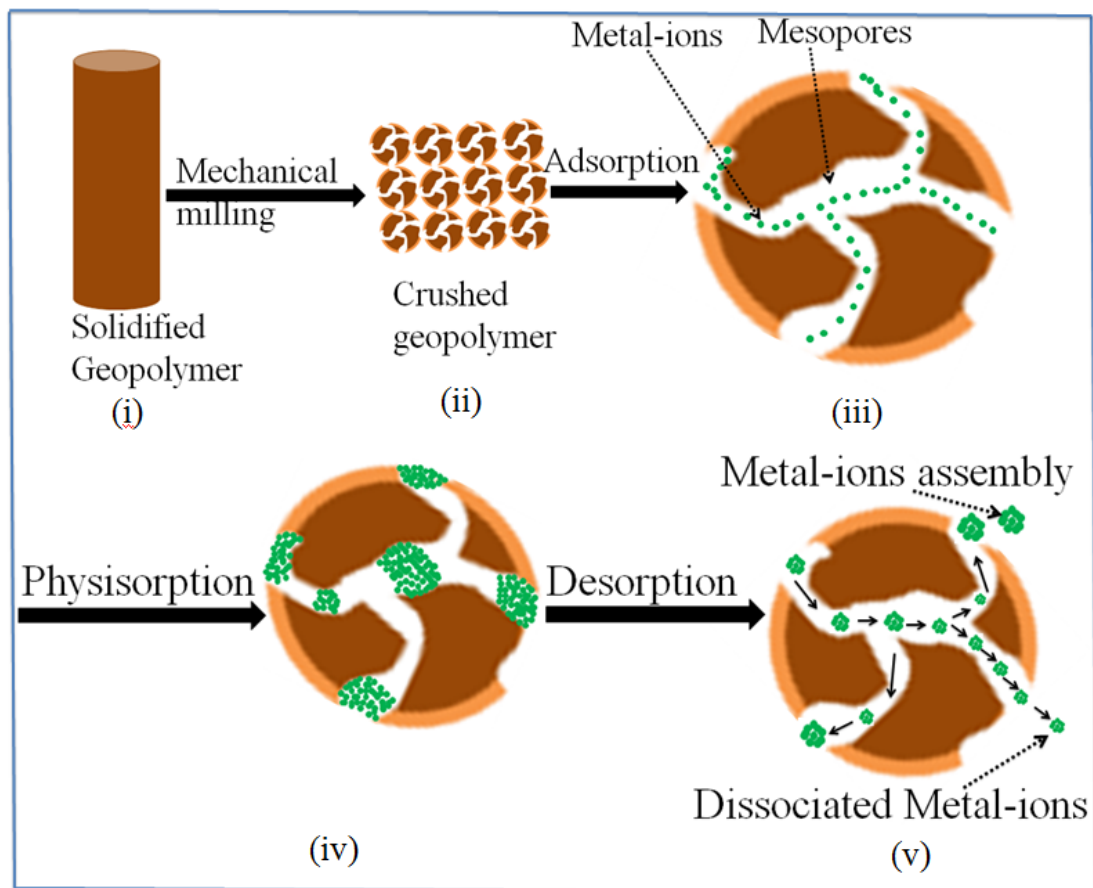


Fig.7

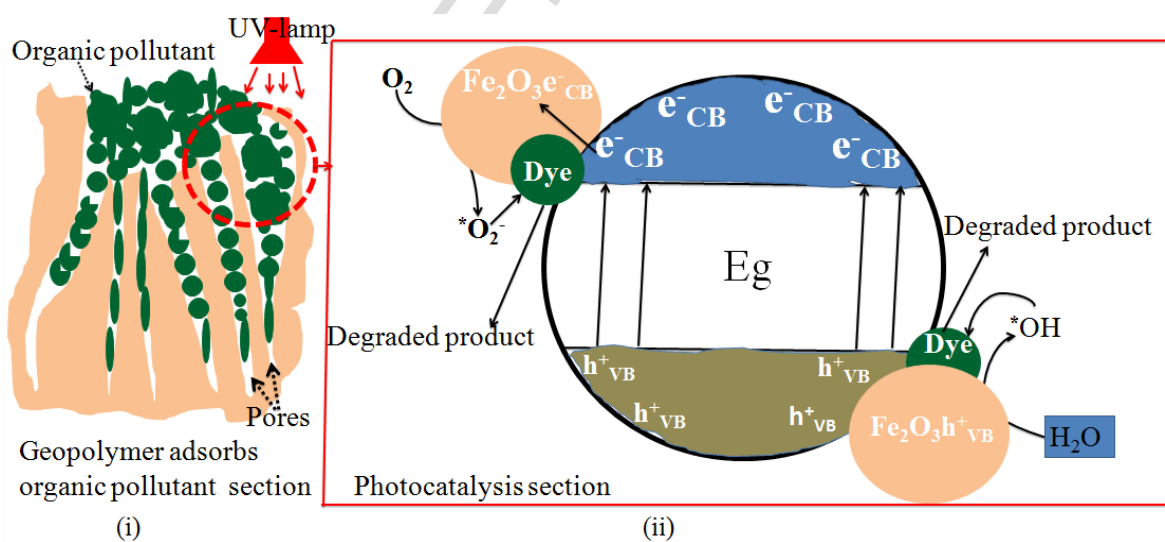


Fig. 8

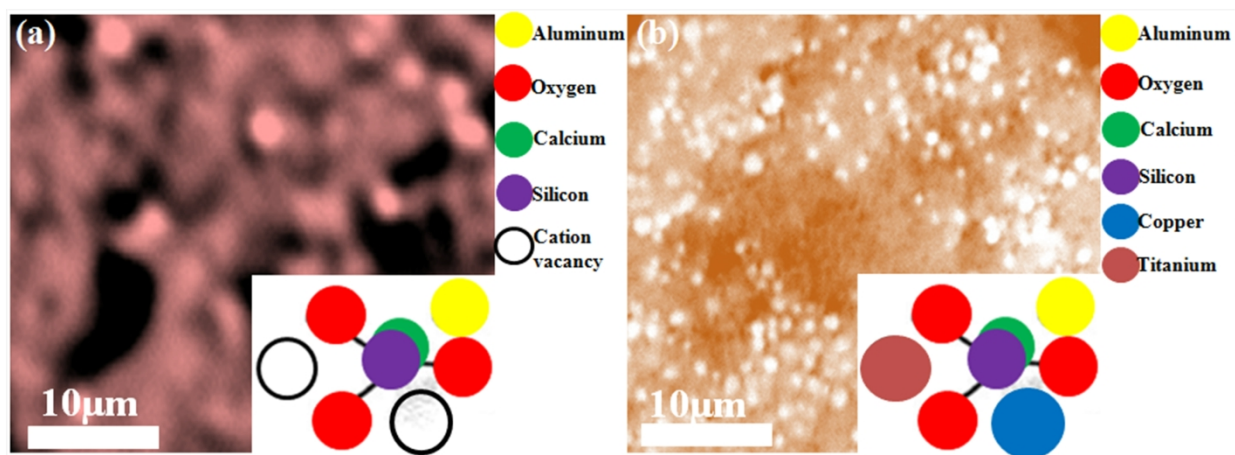


Fig.9

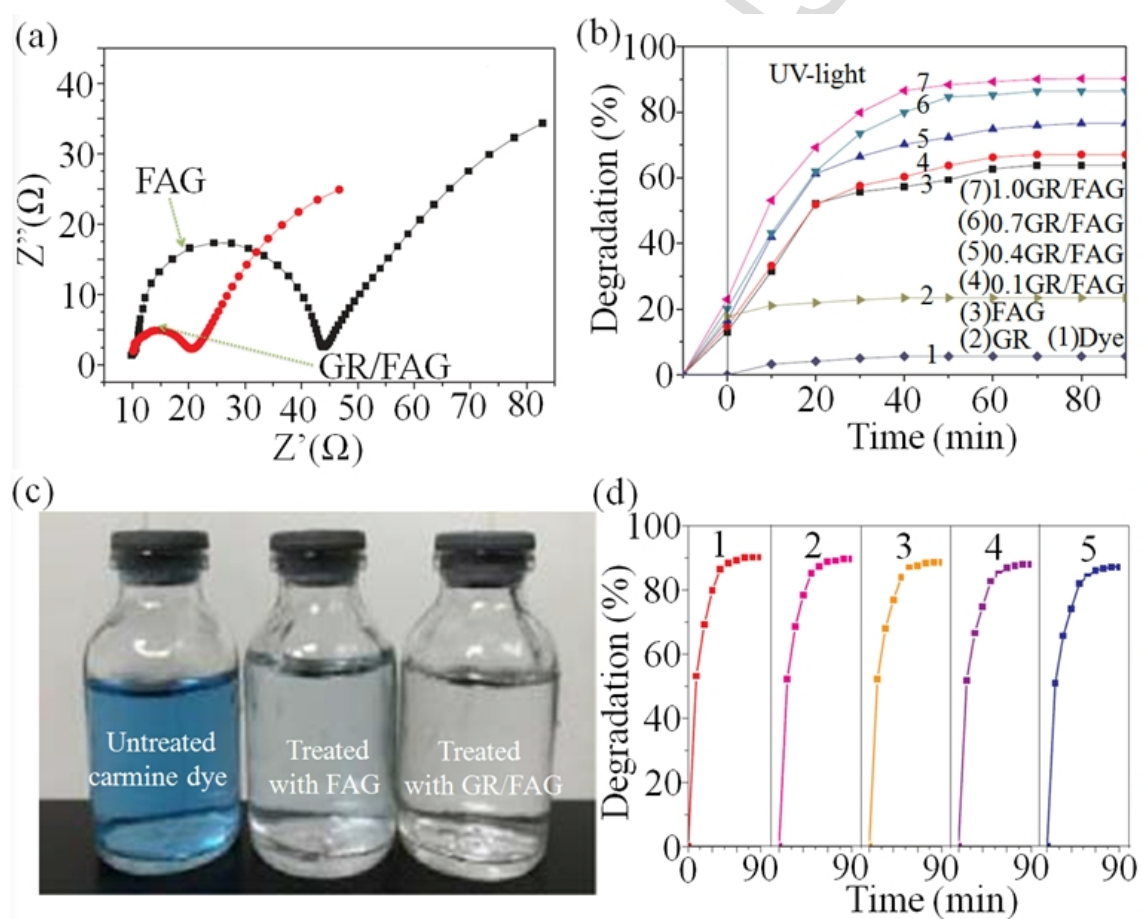


Fig. 10

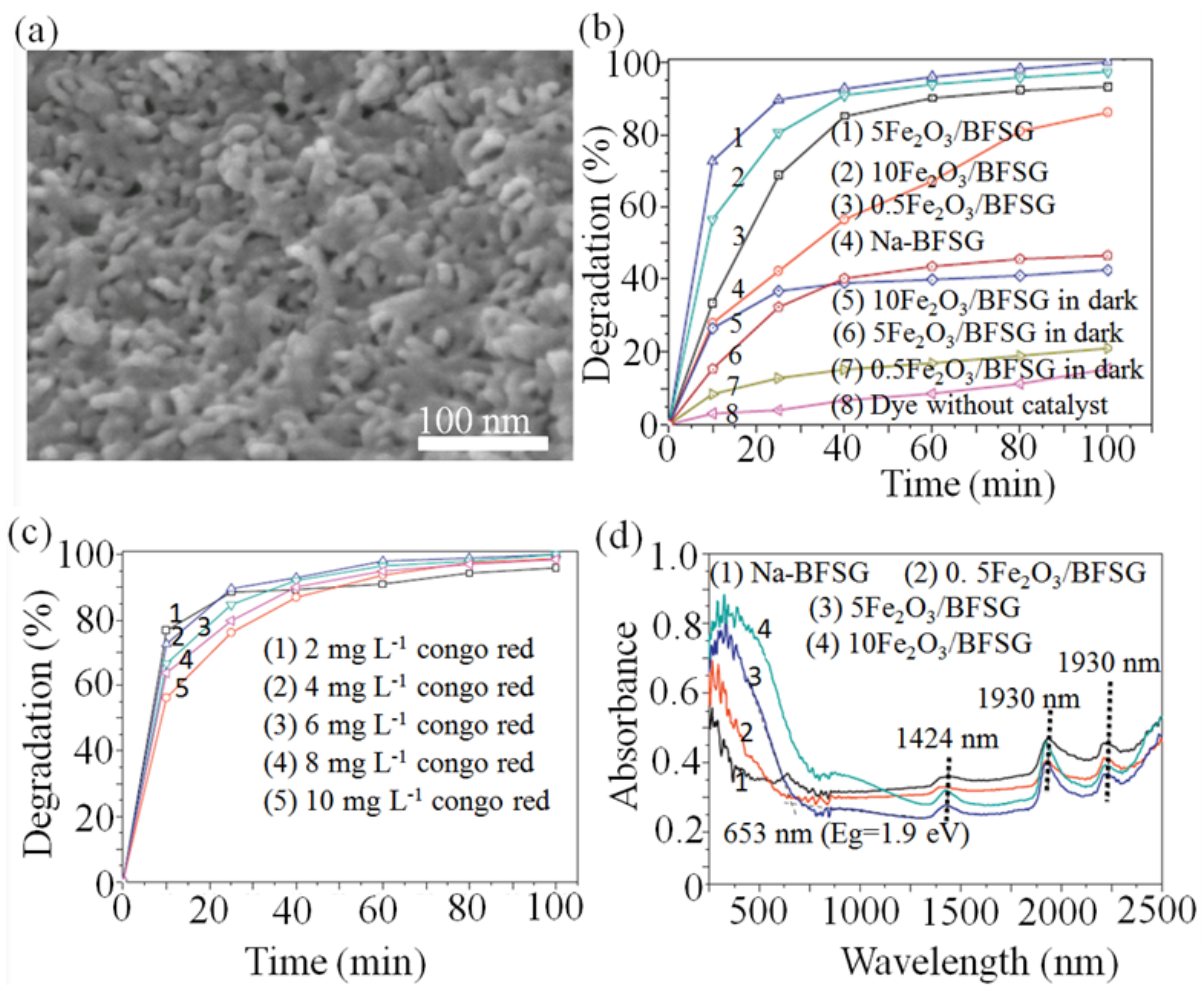


Fig. 11

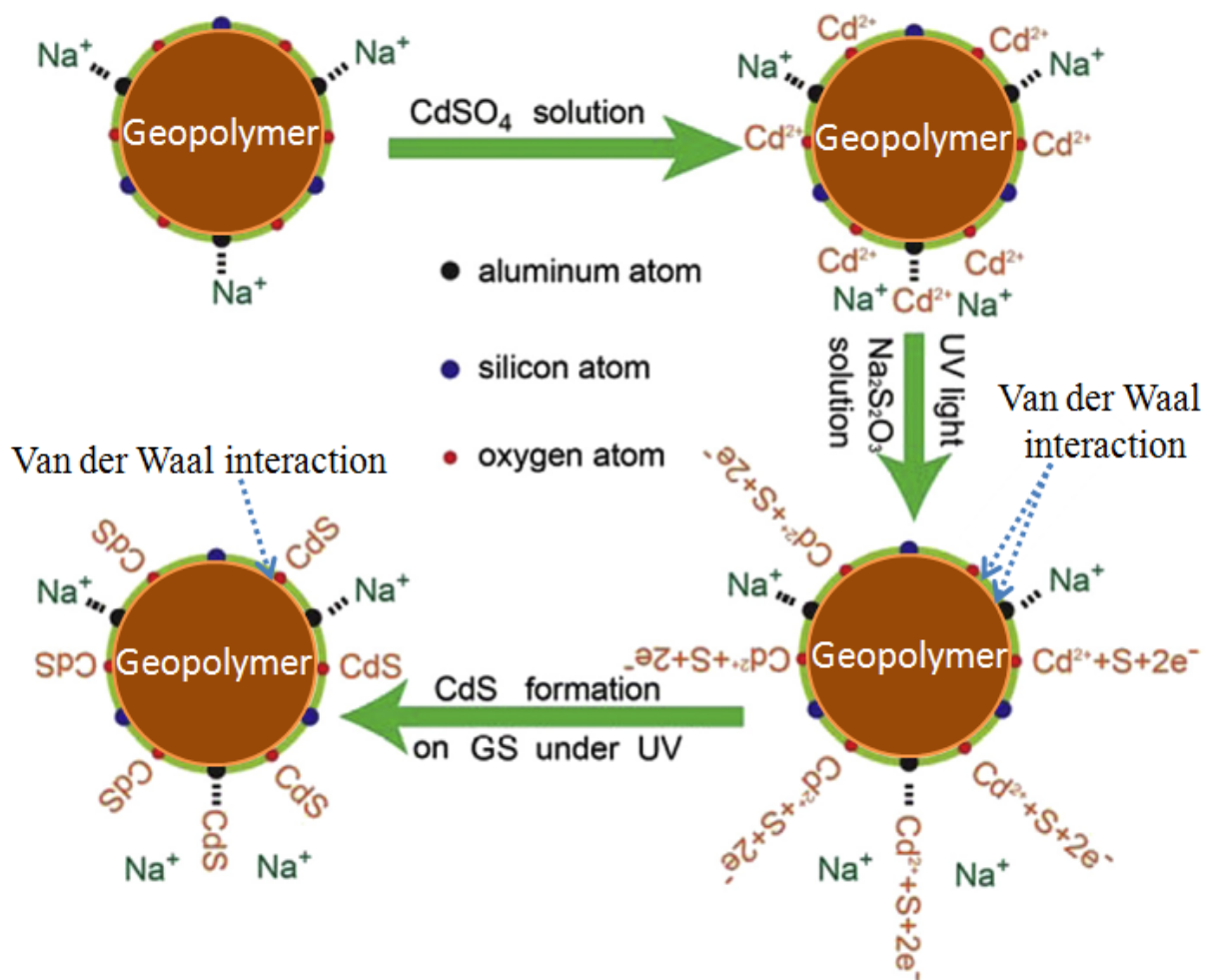


Fig. 12

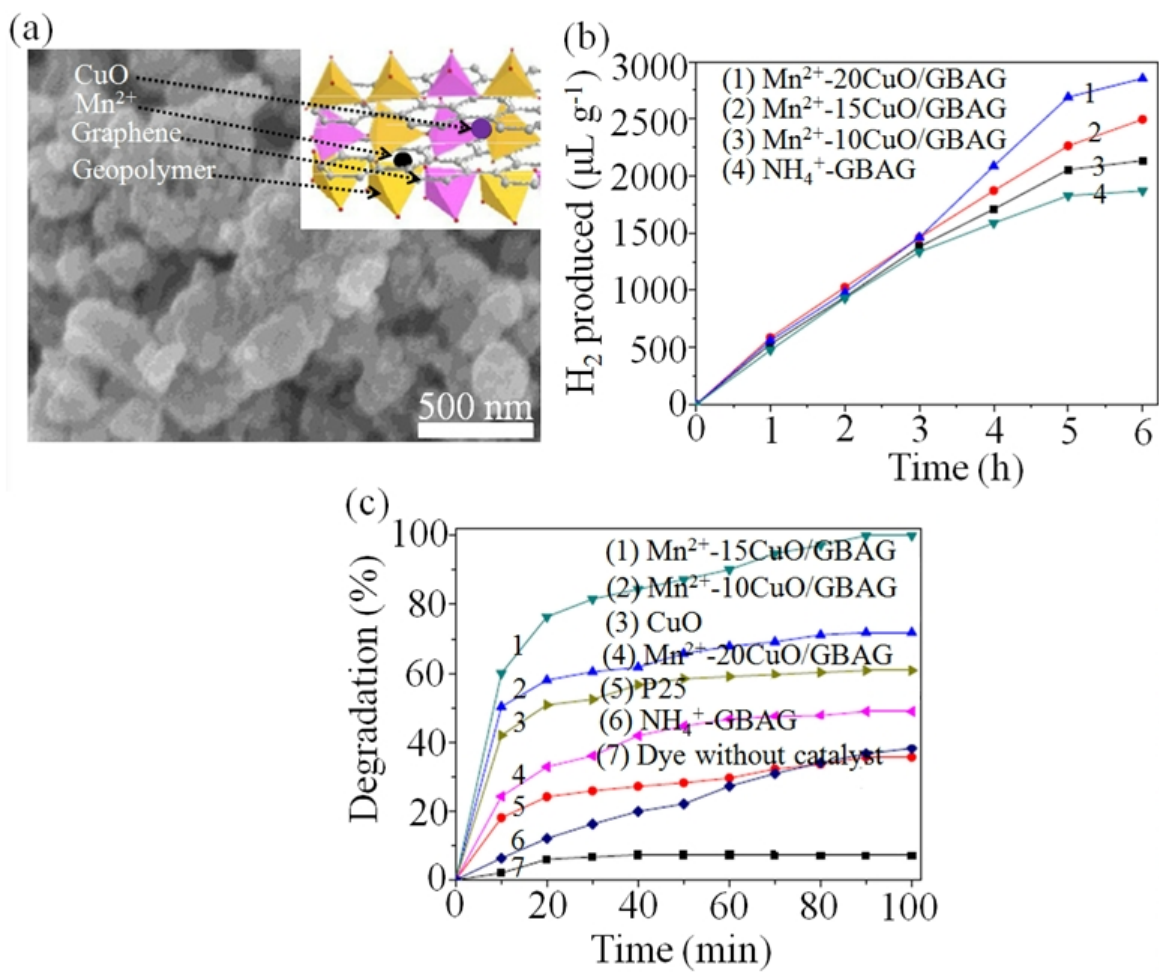


Fig. 13

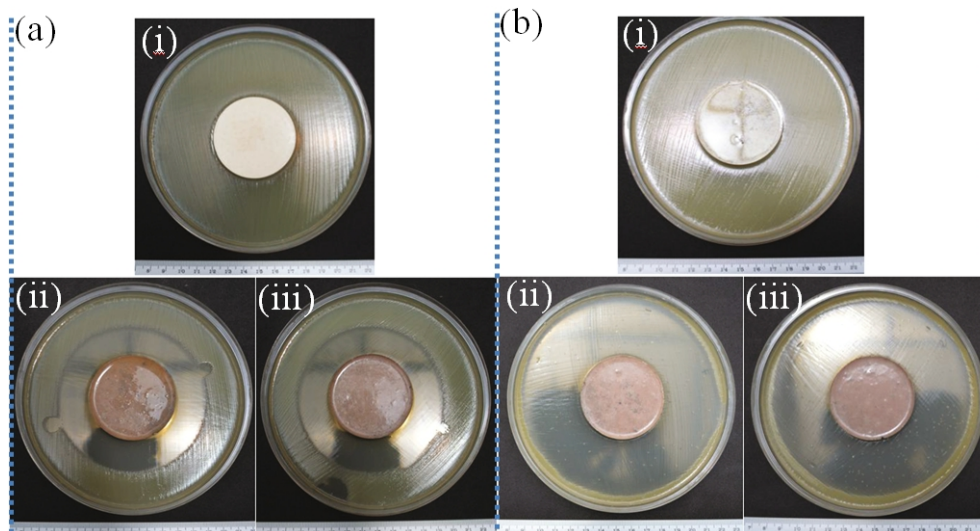


Fig. 14

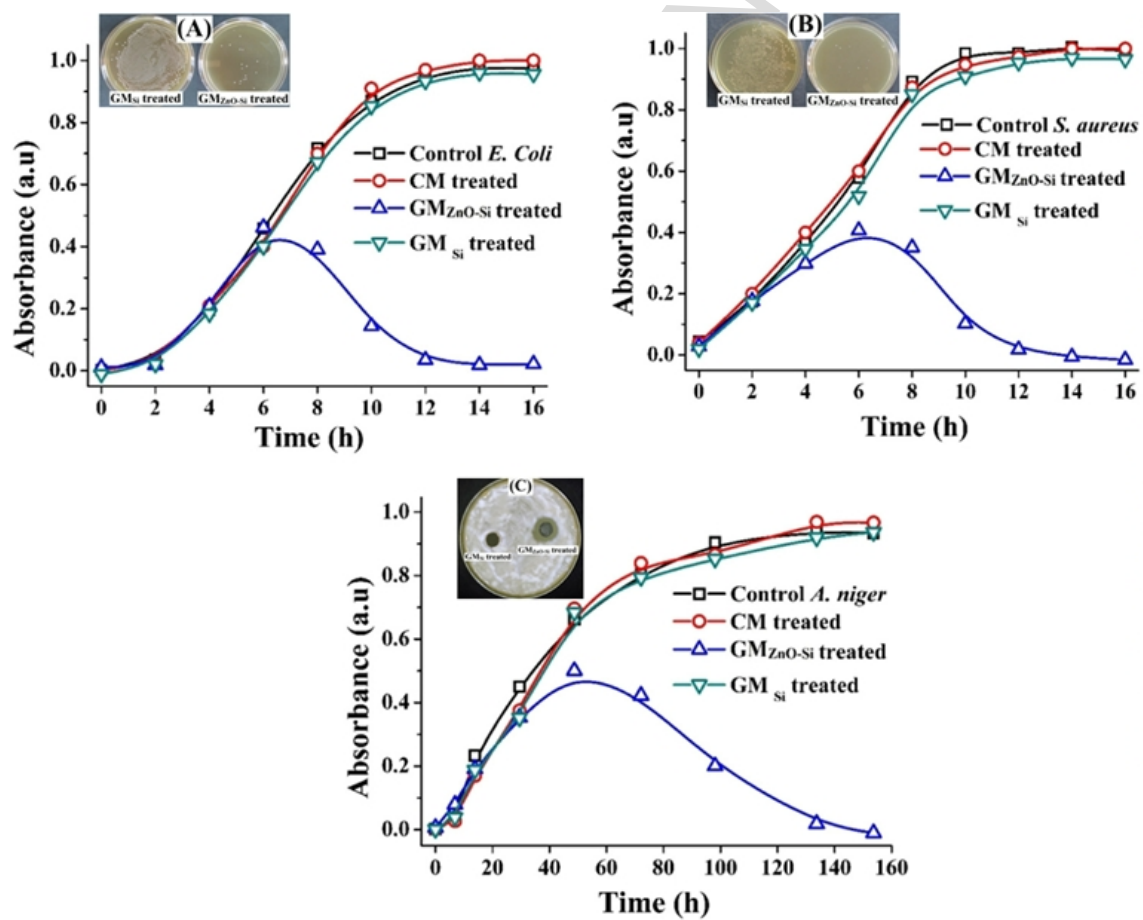


Fig. 15

## Figure captions

**Fig. 1:**

Illustration of geopolymer synthesis and emergent structural framework based on alkaline activator used, and the eventual phase of the final geopolymer.

**Fig. 2:**

Physicochemical comparison of kaolinite, illite, chlorite and montmorillonite as the clay constituents, (Murray 2006) (kaolinite has the most uniform surface and substantial amount of Na/Ca atoms making it a best clay constituent for aiding geopolymerization process). *Adapted from: Murray book.*

**Fig. 3:**

(a) Structural condensation of the kaolinite unit phases. (b) Pseudo-hexagonal sheet of silica (c) octahedral sheet of alumina (Murray 2006). (The pseudo structural phases of both alumina and silica units enable easy dehydroxylation and structural transformation into metakaolin with tetrahedral shape). *Adapted from: Murray book.*

**Fig. 4:**

(a) Stack layer of thermally activated metakaolin. (b) XRD patterns of thermally activated metakaolin at different temperature. (c) FTIR spectra of thermal activated metakaolin at different temperature (Kljajević et al., 2017; Seynou et al., 2016). *Courtesy: (Kljajević et al. and Seynou et al.)*

**Fig. 5:**

Phase mapping of SEM image of fly ash (arrows indicate the distribution of mesoporous metal oxides, quartz which consists of  $\text{SiO}_2$ ,  $\text{Al}_2\text{O}_3$ , and  $\text{CaO}$ , and other constituents) (Kutchko and Kim 2006). *Adapted from: Kutchko and Kim*

**Fig. 6:**

Schematic diagram of blast furnace operation and blast furnace slag production (Chesner, Collins et al. 1998, Saheb 2012). *Courtesy: Saheb et al.*

**Fig. 7:**

Diagrammatical illustration of adsorption and desorption process of metal ions on the surface of geopolymer. {(i) uncrushed geopolymer (ii) geopolymer crushed into nanosphere shapes with small and approximately equal radius size, (iii) transfer of metal-ions through mesopores of the nanosphere geopolymer, (iv) accumulation of the metal-ions onto the adsorption active sites, and (v) desorption of the metal-ions from the surface of geopolymer via simple washing process}.

**Fig. 8:**

Schematic illustration of organic compound photodegradation using geopolymer photocatalysts. (i) Initial adsorption stages of organic molecules, and (ii) photodegradation of adsorbed organic molecules.

**Fig. 9:**

SEM image of (a) undoped geopolymer (inset: geopolymer structural unit with cation vacancy) where the mesoporous surface serves as nanoparticle or cations venues/vacancies, and (b) doped

geopolymer (inset: geopolymer structural unit with the cation substitution), here the porous surface is occupied by CuO and TiO<sub>2</sub> for the cationic exchange and incorporation (Falah, MacKenzie et al. 2016). *Adapted from Falah et al.*

**Fig. 10:**

(a) Electroconductivity of fly-ash based geopolymer and graphene decorated fly-ash-based geopolymer. (b) Photodegradation of indigo carmine dye using various graphene decorated fly ash-based geopolymer, fly ash-based geopolymer, and graphene catalysts, and without catalyst under UV-lamp. (c) Quantitative comparison of indigo carmine dye photodegradation using graphene decorated fly-ash based geopolymer, fly ash-based geopolymer, and without catalyst under UV-light. (d) Regeneration of graphene decorated fly ash based geopolymer as a indigo carmine dye photocatalyst (Zhang, He et al. 2018). (A substantial regeneration is attained due to the synergetic effect between the graphene and geopolymer). *Courtesy: Zhang et. al.*

**Fig. 11:**

(a) SEM images of Fe<sub>2</sub>O<sub>3</sub>/blast furnace slag based geopolymer. (b) Photodegradation of congo red using various Fe<sub>2</sub>O<sub>3</sub>/blast furnace slag based geopolymer, Na-blast furnace slag based geopolymer catalyst, and without using catalyst under UV. (c) Use of 20%Fe<sub>2</sub>O<sub>3</sub>/blast furnace slag based geopolymer photocatalyst as a function of Congo Red concentration. (d) Photoluminescence absorbance of Fe<sub>2</sub>O<sub>3</sub>/blast furnace slag based geopolymer, Na-blast furnace slag based geopolymer (Yao, Li et al. 2013). (A dissolution limit to initiate good electron transfer is established at 5%Fe<sub>2</sub>O<sub>3</sub>@BFSG which shows that the BFSG also has photocatalytic properties) *Courtesy: Yao et. al.*

**Fig. 12:**

Illustration of ionic exchange of Na<sup>+</sup>, K<sup>+</sup>, Ca<sup>2+</sup> of alkaline activator used for geopolymer fabrication with transitional metal-ion for enhancing photocatalytic properties (Li, He et al. 2016). (The presence of weak Van der Waal forces enable easy replacement of alkaline/alkali metal-ions with the photoactive transition metal-ions) *Courtesy: Li et. al.*

**Fig. 13:**

SEM images of Mn<sup>2+</sup>-CuO/graphene decorated geopolymer (inset corresponds to composite distribution). (b) Amount of hydrogen generated against each catalyst. (c) Use of Mn<sup>2+</sup>-CuO/graphene decorated geopolymer, NH<sub>4</sub><sup>+</sup>-geopolymer as a photocatalyst and with catalyst for the degradation of direct sky blue 5B dye under UV light (Zhang, He et al. 2017). *Courtesy: Zhang et. al.*

**Fig. 14:**

(a) (i) Activity evaluation against E. Coli using a standard metakaolin based geopolymer cement without E. Coli inhibition. (ii) A geopolymer cement disk with 0.5% (w/w) of Triclosan against E. Coli and a 90 mm Halo was developed on it. (iii) A geopolymer cement disk with 1.5% (w/w) of Triclosan against E. Coli. A 90 mm Halo was developed on it. B (i) S. aureus activity evaluation of a standard metakaolin based Geopolymer cement disk without bacteria inhibition. (ii) Activity evaluation against S. aureus of a geopolymer cement disk with 0.5% (w/w) of Triclosán. A 116 mm Halo was developed on it. (iii) Activity evaluation against S. aureus of a geopolymer cement disk with 1.5% (w/w) of Triclosán. A 116 mm Halo was also developed on it

(Rubio-Avalos 2018). (Although pure geopolymer shows little or zero inhibition against both gram positive and negative bacteria growth, but it is a good support for the Triclosan for antibacterial activity) *Courtesy: Nur. et al.*

**Fig. 15:**

Mortality studies of the (a) *E. Coli* (b) *S. aureus*, and (c) *A. niger* (inset show the Agar plate/SDA images of microbial strain corresponding to each bacteria)(Sarkar, Maiti et al. 2018). (Use of ZnO-SiO<sub>2</sub> composites to functionalize geopolymer have enhanced activity when compared to single ZnO or SiO<sub>2</sub>) *Courtesy: Sarkar et. al.*

## Highlights

- (i) Raw materials, and (ii) synthetic/process parameters influence geopolymer properties.
- Properties relevant for H<sub>2</sub>-production and photodegradation are elaborated.
- Filler-materials from wastes relevant for catalytic-enhancement are identified.
- Heavy-metal removal using geopolymers: methods and mechanisms are elucidated.
- Technology barriers of relevance to all stake holders are projected.